

LUT UNIVERSITY
School of Energy Systems
Degree Programme in Electrical Engineering

Master's thesis

Matias Huttunen

DESIGN OF BATTERY ENERGY STORAGE FOR HYBRID PASSENGER FERRY

Examiner: Associate Professor Pasi Peltoniemi

Supervisor: M.Sc. (Tech.) Tuomas Talja

ABSTRACT

LUT University
School of Energy Systems
Degree Programme in Electrical Engineering

Matias Huttunen

Design of battery energy storage for hybrid passenger ferry

Master's Thesis

2021

76 pages, 48 Figures, 8 Tables and 1 appendix

Examiner: Associate Professor Pasi Peltoniemi

Supervisor: M.Sc. (Tech.) Tuomas Talja

Keywords: Energy storage, Battery, Lithium ion, Hybrid, Propulsion

Energy storage was designed for ferry operating in over 80 km route in this study. The operation was inspected in two scenarios where in first the energy was used to feed the propulsion to keep the engines in more efficient area of operation and to prevent low load operation. In the second scenario the energy was used to power the hotel load in harbors. The charging of the energy storage was done by using the diesel generators when the load demand was below the 30 % of main engine nominal power so that the low load use of generator is avoided. Initial data for the operation was generated also in this study.

Battery energy storage was selected to be the energy storage technology and the most suitable battery technology for the operation was either LFP or NMC from which the NMC was selected since there are more commercial ready solutions. The capacity of the energy storage was 6 MWh in propulsion scenario and 2 MWh in hotel load scenario. The capacities were optimized so that in the propulsion scenario all the charging power of the low load operation was utilized and in the hotel load scenario the power needed during harbour operation can be fed from the energy storage. Energy storage operation was simulated in the end of lifetime operation when there is 80 % of the initial capacity left. The lowest SoC limit was 20 % so that the batteries were not discharged completely.

Energy storages can be placed either near main engines in separate battery rooms with separate ventilation and fire extinguishing systems or outside decks for more safe operation. Outside deck positioning could be problematic for ship stability point of view. Financially the investment is not profitable because the system will not pay itself back with fuel savings. Component aging and corporate image impact are hard to measure financially so they can be also other drivers for investment, but they were not investigated in this study.

TIIVISTELMÄ

LUT-Yliopisto
School of Energy Systems
Sähkötekniikan koulutusohjelma

Matias Huttunen

Hybridikäyttöisen matkustajalautan akuston suunnittelu

Diplomityö

2021

76 sivua, 48 kuvaa, 8 taulukkoa ja 1 liite

Tarkastaja: Professori Pasi Peltoniemi

Ohjaaja: Diplomi-insinööri Tuomas Talja

Avainsanat: Energiavarasto, Akusto, Litium ioni, Hybridi, Propulsio

Tässä tutkimuksessa suunniteltiin energiavarasto matkustajalautalle, joka liikennöi yli 80 km pituisella reitillä. Laivan operointia tutkittiin kahdessa eri skenaariossa missä ensimmäisessä energiavarastoa käytettiin propulsioon, jolloin pääkoneita pystyttiin pyörittämään paremmalla hyötysuhteella ja vältettäisiin myös alhaisen kuormituksen operointi. Toisessa skenaariossa energia käytettiin hotellikuorman syöttämiseen satamassa. Energiavarasto ladattiin dieselgeneraattoreilla silloin kun kuormitus on alle 30 %, jotta vältetään alhaisen kuormituksen operointi pääkoneilla. Lähtöarvot simulointia varten generoitiin myös tässä työssä.

Akusto valittiin energian varastointitavaksi ja paras akkuteknologia on LFP tai NMC, joista NMC on valikoitu tarkasteluun, koska valmiita kaupallisia ratkaisuja löytyi laajalti. Energiavaraston kapasiteetiksi valikoitui ensimmäisessä skenaariossa 6 MWh propulsiokäytölle ja toisessa skenaariossa 2 MWh hotellikuorman syötölle. Kapasiteetit optimoitiin niin, että kaikki potentiaalinen latausteho saatiin hyödynnettyä pitämään pääkone paremmalla hyötysuhdealueella. Hotellikuorman skenaariossa kapasiteetti mitoitettiin riittämään tarvittavalle energialle satamaoperoinnissa. Energiavaraston simuloinnit toteutettiin energiavaraston käyttöään lopussa, jolloin 80 % kapasiteetista oli käytössä. Alin varaustason raja oli 20 %, jolloin akustoa ei koskaan päästetä purkautumaan kokonaan tyhjäksi.

Akustot voidaan sijoittaa joko pääkoneiden lähistölle alakansille erilliseen akustohuoneeseen erillisellä ilmastoinnilla sekä palosammutusjärjestelmällä varustettuna. Toinen vaihtoehto on sijoittaa akusto ulkokannelle, jolloin sen operointi on vikatilanteessa turvallisempaa, mutta kuitenkin sijoituspaikka saattaa olla laivan vakauden näkökulmasta kriittinen. Taloudellisesti investointi ei ole kannattava, koska se ei maksa itseään koskaan takaisin pelkillä polttoainesäästöillä. Vaikutusta komponenttien ikääntymiselle ja yhtiön imagolle on vaikea mitata rahassa, mutta nämä voisivat myös olla syitä investoinnille, niitä ei kuitenkaan tutkittu.

TABLE OF CONTENT

1.	INTRODUCTION.....	8
2.	HYBRID PASSENGER FERRY.....	9
2.1	Largest battery energy storages in ships	9
2.2	Electric distribution structure.....	9
3.	DEFINITION OF BASE VALUES	12
3.1	Route of operation	12
3.2	Size of the ferry	14
3.3	Propellers and propulsion technologies	15
3.3.1	Fixed pitch propellers	15
3.3.2	Controllable pitch propellers.....	16
3.3.3	Podded and azimuth propulsion	17
3.3.4	Transverse thrusters	18
3.3.5	Ducted propellers.....	18
3.3.6	Contra-rotating propellers	19
3.4	Propulsion power.....	20
3.5	Electrical energy consumption.....	28
3.6	Main engines and generator sets	30
4.	ELECTRICAL ENERGY STORAGE.....	33
4.1	Energy storage options	33
4.2	Battery materials.....	34
4.2.1	Lithium Nickel Cobalt Aluminium Oxide	36
4.2.2	Lithium Nickel Manganese Cobalt Oxide	37
4.2.3	Lithium Iron Phosphate.....	38
4.2.4	Lithium Titanate	39
4.3	Comparison of lithium batteries.....	41
4.4	Control methods	41
4.5	Regulations and classifications	43
4.5.1	Ventilation.....	43
4.5.2	Fire safety.....	44
5.	DESIGN OF THE BATTERY ENERGY STORAGE SYSTEM.....	45
5.1	Energy storage operation possibilities	45

5.2	Propulsion assistant energy storage.....	45
5.3	Hotel load serving harbour operated energy storage.....	51
5.4	Battery technology selections	55
5.5	Space requirements for the energy storage	58
5.6	Fuel consumption	60
5.7	Electrical distribution	62
5.8	Cost estimation of the system	63
6.	CONCLUSIONS.....	66
	REFERENCES	68
	APPENDICES	75
	Appendix 1. Simulation model.....	75

ABBREVIATIONS AND SYMBOLS

A_{vs}	Projected area of the ship above the waterline to the transverse plane
BMS	Battery Management System
C	C-rate
C_A	Correlation allowance
C_{AA}	Air resistance coefficient
C_{DA}	Air drag coefficient
C_F	Frictional resistance coefficient
C_T	Total resistance coefficient
C_W	Wave resistance coefficient
DoD	Depth of Discharge
E_{cap}	Total capacity of the energy storage
EFC	Equivalent Full Cycle
FC	Fuel Consumption
GT	Gross Tonnage
IMO	International Maritime Organization
k	Roughness of the hull surface
k_{sm}	Sea margin
LFP	Lithium iron phosphate
LNG	Liquid Natural Gas
L_{pp}	Length between perpendiculars
LTO	Lithium Titanate Oxide
L_{WL}	Length on the designed waterline
NCA	Nickel Cobalt Aluminium oxide
NMC	Nickel Manganese Cobalt oxide
P	Power charged or discharged
P_D	Delivered power
P_E	Effective power
PMS	Power Management System
P_S	Service power

PTI	Power Take In
PTO	Power Take Out
QPC	Quasi-Propulsive Coefficient
R_e	Reynolds number
Ro-Ro	Roll-on/Roll-off
Ro-pax	Roll-on/Roll-off passenger
S	Wetted surface of the ship
SFC	Specific Fuel Consumption
SOC	State of Charge
SOLAS	Safety of Life at Sea
UPS	Uninterruptible Power Supply
v_s	Speed of the ship
ΔC_F	Roughness allowance
η_T	Transmission efficiency
ν	Viscosity of water
ρ_A	Density of air
ρ_w	Density of water

1. INTRODUCTION

Shipbuilding technology is nowadays going towards a point where greener appearance and technology is required. The common opinion of emission reductions affects many transportation, technology and industrial business. In maritime transportation business, produced CO₂ emissions are 940 million tons, which equals 2.5 % of total greenhouse gas emissions and 13 % of the whole transport sector. There is prediction that without reduction actions these CO₂ emissions could increase between 50 % and 250 % until 2050. (European Commission, 2019)

To achieve emission regulations in the future there might be a need for alternative solutions than just a cleaner fuel. Shipowners might need to reconsider the ship operations in case of zero emissions zones become common trend. For example, Norway has created a zero-emission zone where the operation is needed to be emission free before 2026 (Imarest, 2018). Emission reduction trend might push other countries as well for similar solutions which will affect future projects and existing ships. Hybrid solutions in ships offer a way to improve ship operation.

The main purpose of this study is to research the possibilities of using energy storage in passenger ferry for a long route of operation and generate the operation electrical loading data for the inspection. The operation modes are selected so that the battery operation is inspected in sea operation and harbour operation. From these operation modes the benefits are inspected and reviewed. Benefits could be energy savings and fuel savings, financial savings due maintenance costs and emission costs or greener image for the shipowner. The energy storage is designed and dimensioned for the operation after reviewing the options and possibilities. It is assumed that the energy storage will be powered from generators only, so no shore connection is included in this study. Financial aspect of the energy storage implementation is also investigated after providing a solution.

2. HYBRID PASSENGER FERRY

Roll-on/Roll-off passenger (Ro-pax) and Roll-on/Roll-off (Ro-Ro) ferries are used to transfer cargo, vehicles and passengers at the same time. These vessels usually have a few car decks which are located just above the engine rooms. The very first Ro-Ro ferries were invented to carry trains across wide rivers (IMO, n.d.)

In hybrid ships there are at least two different technologies used for electrical loads. There are main engines running with fuel which is usually the primary source of energy and supporting ones could be for example batteries, fuel cells, wind power or solar panels. The main purpose of hybrid concept ship is to lower the fuel consumptions.

2.1 Largest battery energy storages in ships

In ship industry the large energy storages are still quite new thing. The largest projects in development are Corvus retrofit supply of 10 MWh to AIDAPerla and newbuild of Yara Birkeland with 7 to 9 MWh battery energy storage. However, these are not yet in operation and cannot be count as ready products. (IEEE Spectrum, 2021)

The largest hybrid vessels with battery energy storage in operation are ForSea Tycho Brahe and ForSea Aurora with 4.16 MWh battery energy storage retrofitted both in 2017. Tycho Brahe energy storage is going to be updated to 6.4 MWh which will make it the largest installed battery pack in operating vessel. Scandlines also has two ferries with 2.6 MWh energy storages and few others with smaller capacity. (ForSea, 2021, Scandlines, n.d.)

2.2 Electric distribution structure

The ship electric distribution network is commonly in radial power network structure. The radial power distribution is used in in both the mechanical driven ships and hybrid and fully electrical ships. There is also more recent distribution structure where the power distribution is zonal. The largest electrical load in the ship is propulsion which is used to move ship forward. (Shagar, 2017)

Radial distribution is the traditional solution for ship electrical distribution network. In the radial power network structure, the generators supply the main buses which are connected

to the main switchboards and to the loads. Traditional ship high voltage to low voltage radial distribution system structure is shown in Figure 1. (Shagar, 2017)

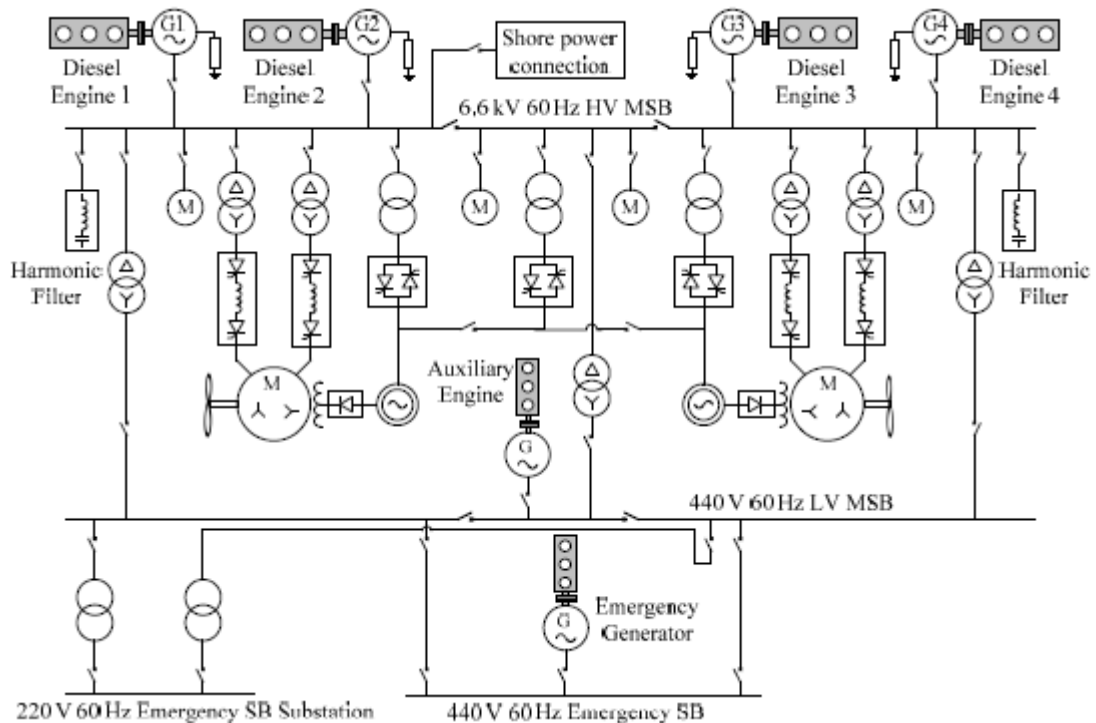


Figure 1. Traditional ship high voltage to low voltage radial distribution system structure (Shagar, 2017)

In modern distribution system topologies, the zonal power distribution is growing its share and the distribution system structures could be moving towards them in the future. There could be AC or DC zonal distribution. These differ from each other mainly so that in AC zonal distribution there is no AC to DC rectification after generated AC electricity. Zonal distribution improves reliability of the distribution system by dividing the distribution into a multiple zones which simplifies the operation during a fault situation. Each zone has its own power source to be able to operate in island conditions. During fault in the system the fault point is isolated by opening the load terminal shown in Figure 2. (Jayasinghe, 2017 & Shagar, 2017)

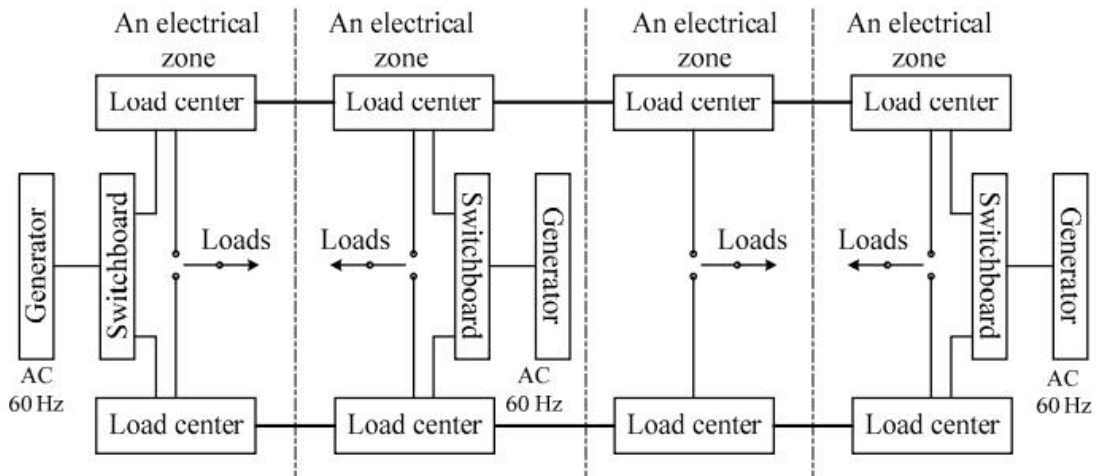


Figure 2. Radial power distribution network topology (Shagar, 2017)

In zonal distribution there is always redundant distribution route for non-fault locations while in the radial distribution one part of the grid is lost during the fault. Zonal distribution requires advanced fault detection, identification and isolation algorithms to be able to isolate the fault from the rest of the grid. (Jayasinghe, 2017 & Shagar, 2017)

In chapter 3 the base values for the operation are defined so that the energy storage can be dimensioned. Energy storage technologies and hybrid usages are further investigated in chapters 4 and 5 where also the used power distribution network structure is presented.

3. DEFINITION OF BASE VALUES

In this case study, there is no existing real ship data available for the design of the energy storage. The data is generated by calculating necessary propulsion power for the route of operation and predicting the hotel load. The main attributes affecting the operation of the ferry is determined using similar reference ship and scaling the necessary values. Then the powers of main components such as main engines, generator sets, and propulsion gear are selected.

3.1 Route of operation

The selected route of operation is between the ports of West Harbour in Helsinki and Old City Harbour in Tallinn. The length of the sea route is 44.2 nautical miles which equals 81.7 km. Most of the route is open sea as seen in Figure 3 but in the archipelago of Helsinki there is slightly more difficult fairway. (Openseamap, 2021)

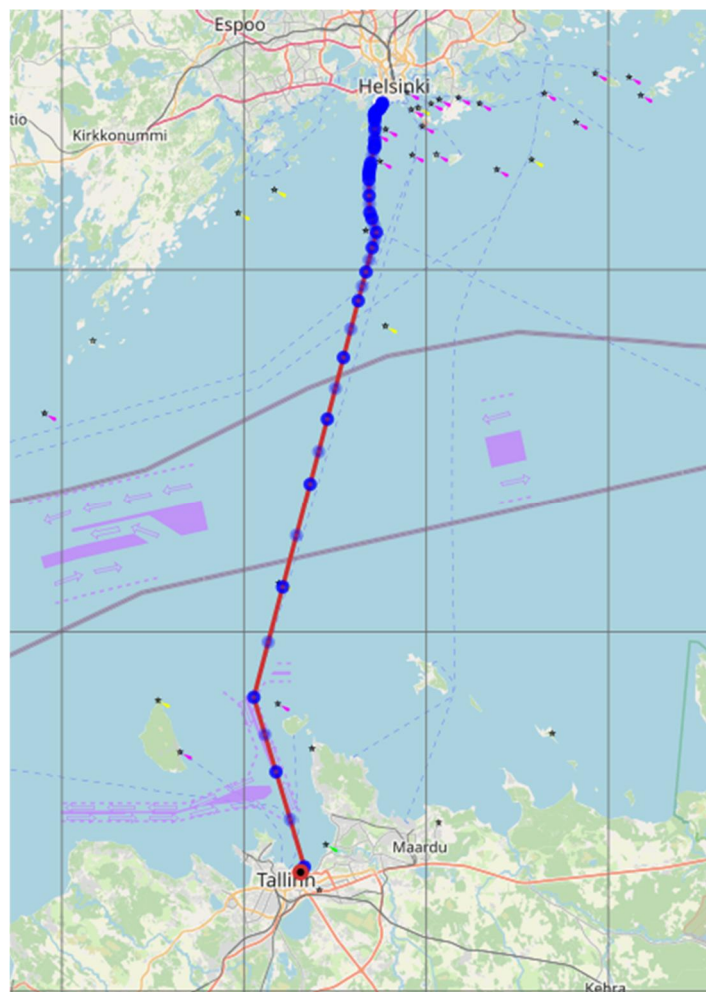


Figure 3. The operation route of the ferry (Openseamap, 2021)

In this operation route there is speed restrictions in the archipelago of Helsinki. This speed restriction area is defined to start from the latitude of $60^{\circ}06'$ N from near Katajaluoto to north towards West Harbour (Figure 4).

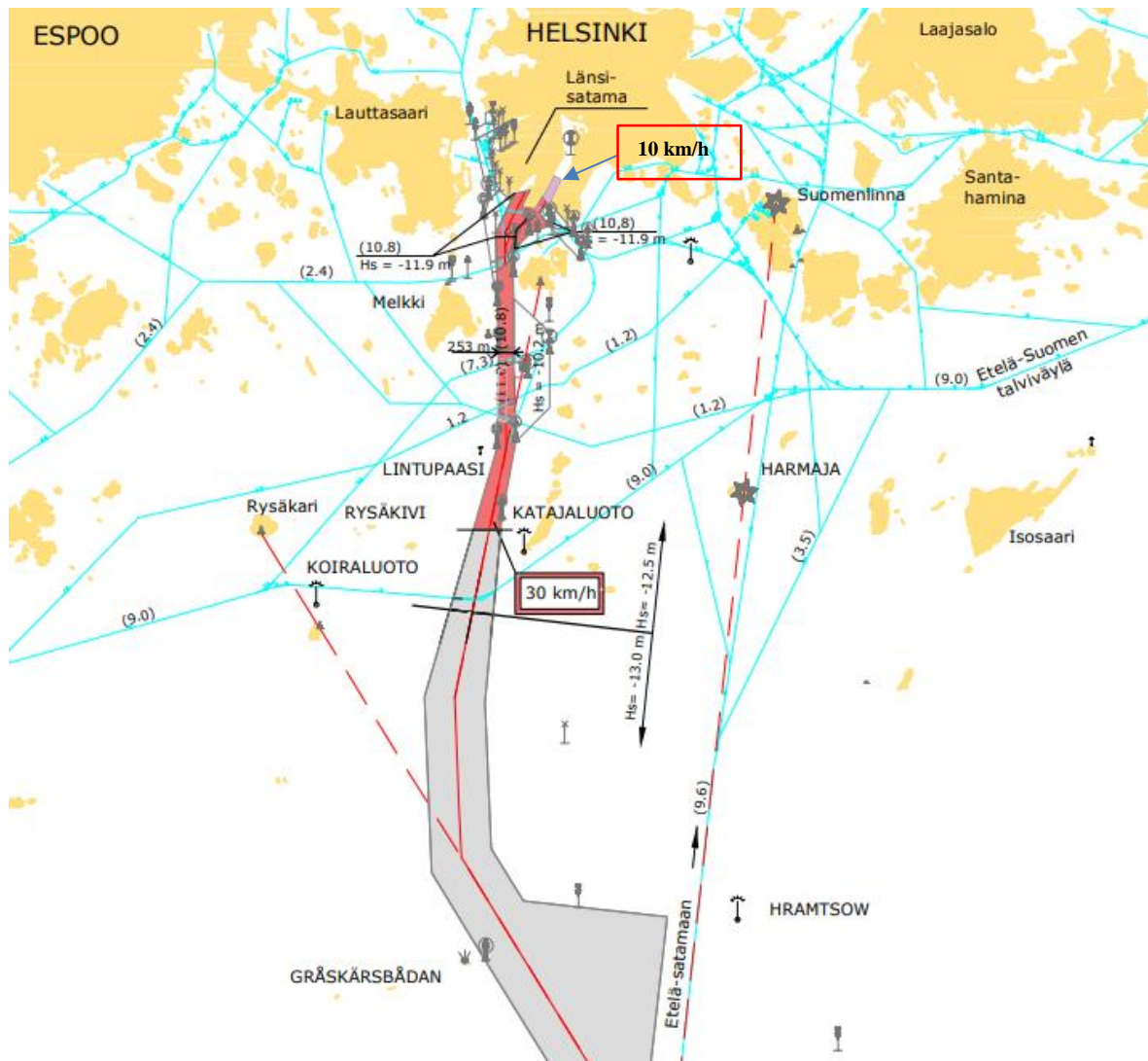


Figure 4. Speed restrictions in the archipelago of Helsinki (Väylävirasto, 2019)

The speed restriction area is 3.3 nautical miles from which 3.1 nautical miles has limited speed of 30 km/h and very short distance in the harbour area has 10 km/h speed limit. (Openseamap 2021 & Väylävirasto, 2019)

After the speed restriction area is bypassed, there are no specific speed limits set. However, in the Old City Harbour of Tallinn port rules there are said that in the port waters the vessel shall be moved at the minimum speed which allows the manoeuvrability of the vessel with steer. Practically this is hard to specify in this work since port water area is not clearly described so the speed limit in the Tallinn harbour is neglected. (Tallinna Sadam, 2020)

3.2 Size of the ferry

The ship size is determined so that the reference ship is selected to get the approximate sizes and then the ship is considered as its own new design. The reference ship is RoPax ferry M/V Kronprins Frederik from Scanlines. The properties and values of the reference ferry is adjusted for this design. The general arrangement of the new ferry is shown in Figure 5. The size of the ship is rounded to 16 000 gross tonnage (GT) which is almost the same as the reference ferry (Scanlines, n.d.). The length is 142 m which is slightly less than reference length, but the ship geometry is a bit different, so the shorter length compensates approximately the differences in hull design.

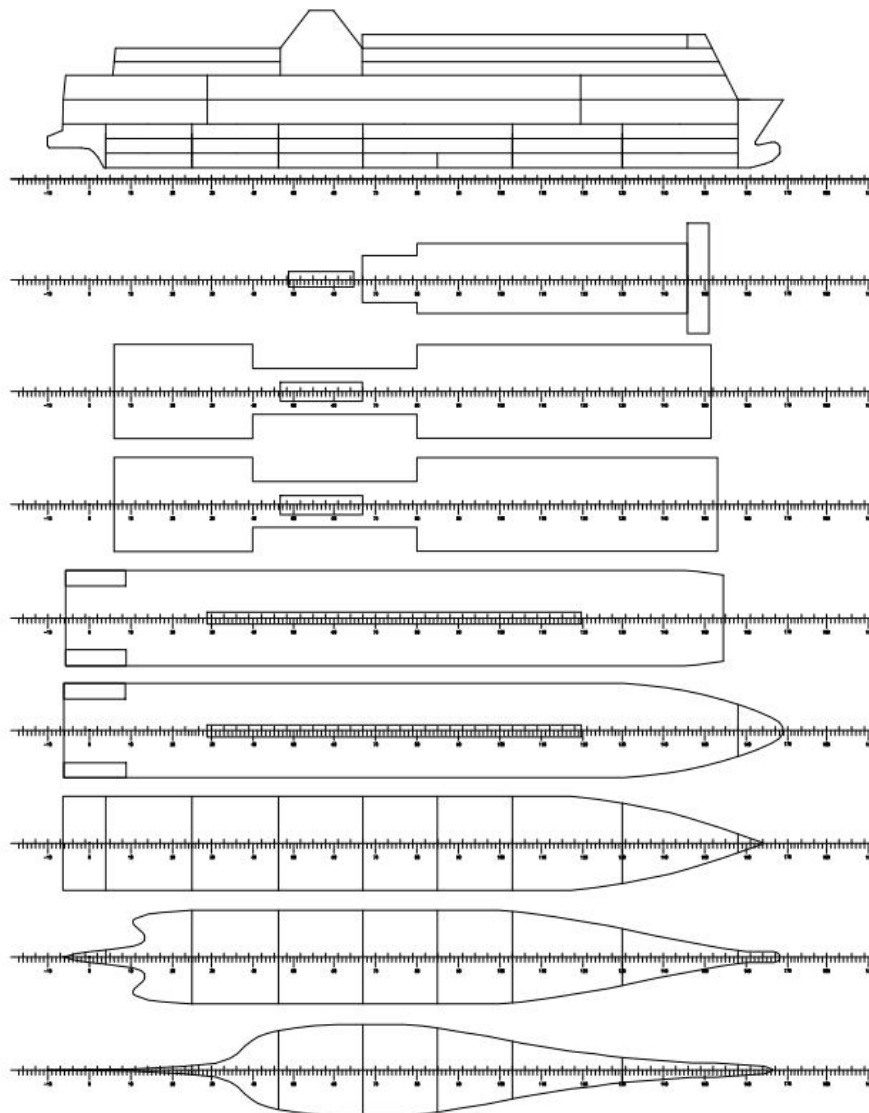


Figure 5. General arrangement of the designed ferry (Papanikolaou, 2017)

The ferry has eight decks shown in Figure 5. The highest deck contains bridge where the ship is operated and some passenger area. Two decks below this are passenger area and cabins, next two has room for cargo such as trucks or other vehicles. Remaining three decks below these car decks contains engine rooms and other machinery spaces that ensures safe and continuous operation of the ferry. The energy storage will be located in the lowest decks near the main switchboards and is further inspected later.

3.3 Propellers and propulsion technologies

For manoeuvring operation of the ship there are multiple options which basically all are based on propeller operation excluding waterjets. The propeller can be connected either to electrical motor, generator or mechanically to main engine. The rotating propeller accelerates water causing a thrust effect and ship movement. From these propeller technologies the most used one is fixed pitch propeller. The propeller itself can be a mono-block or built-up propeller in which mono-block propeller is commonly used these days. Figuratively the mono-blocks are cast as a single block and the built-up propeller has every blade bolted separately from flange to shaft. These built-up propellers are beneficial in such ship operation that depends on a time schedule or is operated in such area or environments where the propeller could get damaged easily. One blade is cheaper to change rather than the whole block and needs no dry docking since it can be changed underwater. (Carlton, 2012; Molland, 2011 & Wärtsilä, n.d.)

The selection of the propeller and propulsion technology has an effect to energy efficiency which directly affects to electrical energy consumption and therefore into the design of the energy storage.

3.3.1 Fixed pitch propellers

As mentioned earlier the fixed pitch propeller is the most commonly used propeller technology. In fixed pitch propellers the pitch angle is optimized at the design phase to work as energy efficient as possible. Other important factors are reduction of vibration excitation and the effect of radiated noise on marine mammals and fish. Pitch angles cannot be adjusted in operation as in controllable pitch propellers. In Figure 6 is shown built-up fixed pitch propeller. This is also the propeller technology used in the model ship. (Carlton, 2012)



Figure 6. Built-up fixed pitch propeller (Wärtsilä, n.d. a)

Larger propellers are cast usually in non-ferrous materials such as high-tensile brass with manganese and nickel-aluminium bronzes. Stainless steel is also used for large propellers. For the small propellers polymers, aluminium, fiber carbon and nylon are used. Blade numbers are selected so that the cavitation effect is controlled. Usually, the blade numbers vary from two to seven blades so that the pleasure crafts use two to three blade propellers, tugs and fishing boats three bladed design and merchant vessels four to seven blades. Rudders are used after the propeller to control the manoeuvring. (Carlton, 2012)

3.3.2 Controllable pitch propellers

Controllable pitch propellers allow pitch angle optimization depending on propeller load conditions. The control of pitch angle allows more efficient operation which leads to less cavitation. Controllable pitch propellers are more mechanically complex than fixed pitch propellers. The propellers are also more expensive and have larger maintenance costs than

in fixed pitch propellers. Often these propellers are used in passenger ships, cargo, tugs, trawlers and ferries since the operating conditions benefit from the pitch angle control. Benefits are fine thrust control in manoeuvring or in dynamic positioning. (Carlton, 2012 & Molland, 2011)

3.3.3 Podded and azimuth propulsion

Podded propulsion is a fixed-pitch propeller variant where propeller is located in a pod that can be rotated 360 degree in azimuth direction. Podded propulsion required no rudder since the pod rotation controls the thrust direction. Commonly the podded propulsion is used in cruise ships and ice breakers because of the manoeuvrability advantages. Basic concept of podded propeller is presented in Figure 7. (Carlton, 2012 & Molland, 2011)

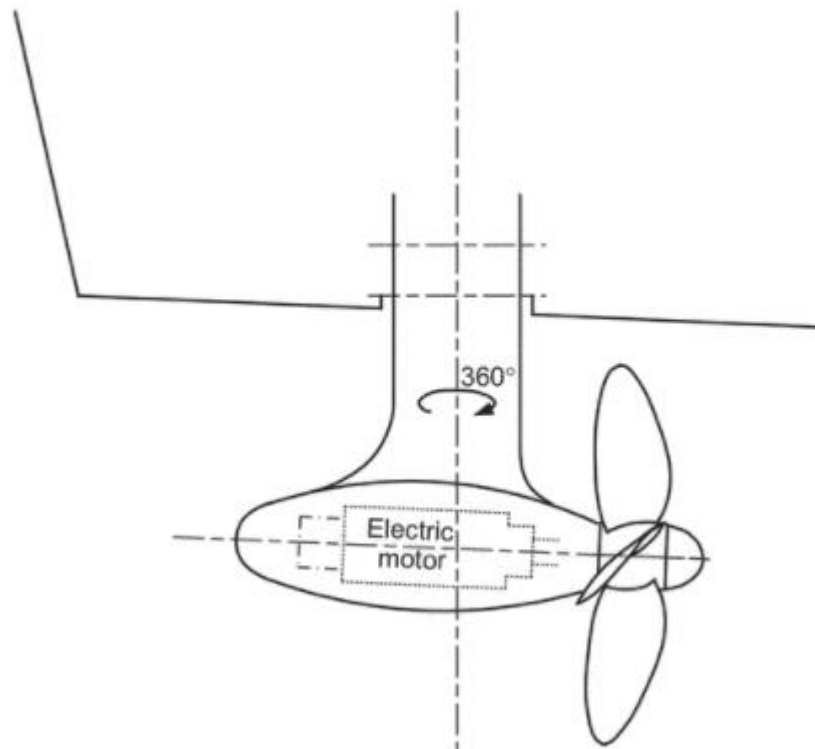


Figure 7. Podded propeller (Molland, 2011)

If the propeller is in the front of the pod the term used is puller or tractor and if the propeller is in the end of the pod the term is pusher. Podded propulsion is called azimuth propulsion if the electric motor that drives the propeller is located inside the ship hull rather than inside the pod. In these cases, the mechanical drive shaft which is Z or L type operates the propeller. (Carlton, 2012 & Molland, 2011)

3.3.4 Transverse thrusters

Transverse, lateral or tunnel thrusters are usually used in harbour operation where low speed side movement is required. They are used in auxiliary applications and ship requires also other propulsion technology to be able to move forward. Bow thrusters are located in the front of the ship and stern thrusters in the aft ship. Lateral thrusters are fitted inside the hull so that the propeller moves the water sideways (Figure 8). (Molland, 2011)

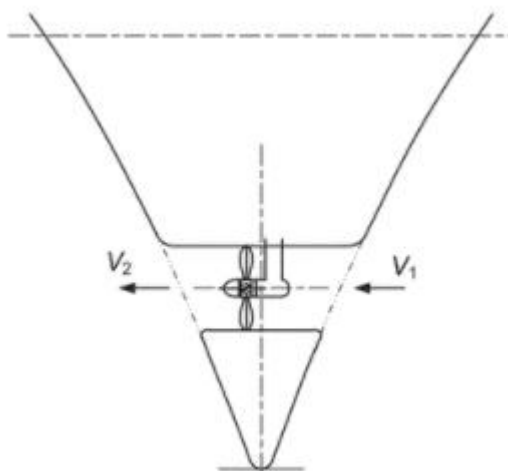


Figure 8. Lateral bow thruster unit (Molland, 2011)

For model ship the bow thrusters are dimensioned with estimation that the thruster power for ferries is from 0.54 kW/m^2 to 0.96 kW/m^2 but usually around 0.6 kW/m^2 to 0.8 kW/m^2 according to Wärtsilä. In this study the model ship side wind area is approximately 2420 m^2 and the used thruster power is decided to be nominal of 1400 kW . This means that the used thrusters are in the dimension estimation range with the power being approximately 0.58 kW/m^2 . (Wärtsilä, n.d. b)

3.3.5 Ducted propellers

In ducted propellers there are two types of designs which are accelerating and decelerating duct propeller. Accelerating duct accelerates the water flow inside the duct providing higher efficiency in high thrust load conditions. This comes practical in tugs when towing large masses or in trawlers when trawling. It can also be rotated for steering. However, the efficiency in free-running and light load operations is less than the efficiency of a non-ducted propeller. The opposite of the accelerating duct, decelerating duct propeller reduces the flow speed inside the duct. It increases the pressure at the propeller to reduce the cavitation and noise radiation. Decelerating duct propeller is good for instances where the noise is needed

to keep in minimum. The good example for these is military craft where minimizing the cavitation noise is important factor. In the Figure 9 there is first shown accelerating duct propeller and then decelerating duct propeller. (Carlton, 2012 & Molland, 2011)

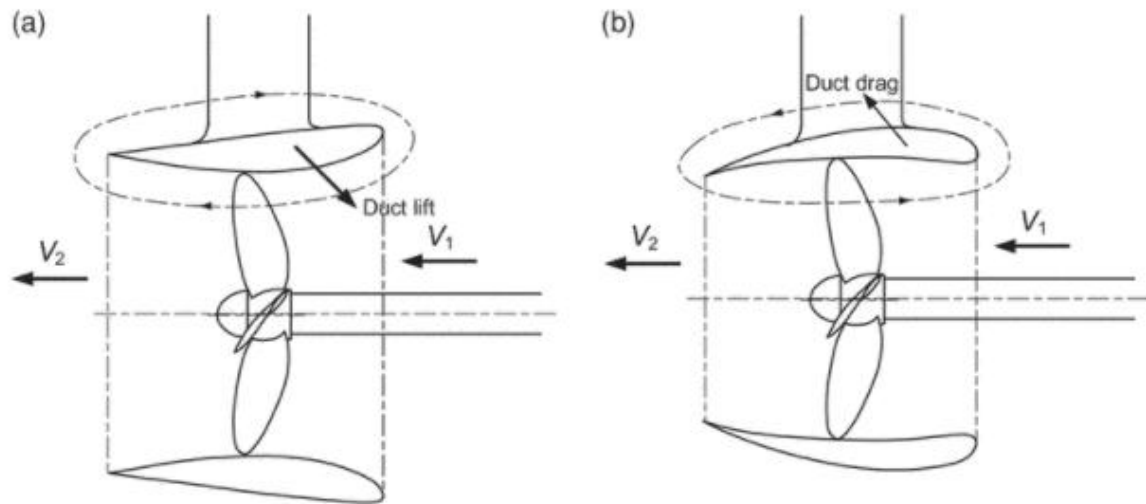


Figure 9. Accelerating duct propeller (a) and decelerating duct propeller (b) (Molland, 2011)

The theory behind ducted propeller can be defined with incompressible flow in a closed conduit between two stations where the product of cross section area, velocity and density in the first point equals the same product in the second point. In the accelerating duct the cross section of the inlet is larger than the cross section of the outlet so the outlet velocity must be higher since water is incompressible and density remains constant. In the decelerating duct the induced velocities of the propeller are taken into account for the velocity distribution through the duct. The duct has a slight inside curve where the cross section is slightly increased from inlet to propeller where the velocity decreases. After propeller the cross section is slightly smaller where the pressure and velocity rises again. (Carlton, 2012)

3.3.6 Contra-rotating propellers

In contra-rotating propeller there are two coaxial propellers that rotate in different directions. The propeller located in aft has a smaller diameter and usually more blades than the propeller in front. The propeller in aft benefits from the slipstream contraction of the front propeller. The contra-rotating propeller arrangement also stabilizes the torque reaction making it a good technology for torpedoes and high-speed solutions. Contra-rotating propulsion technology also has a variant solution installed in for example in two ferries in Japan shown in

Figure 10 where front propeller is shaft-driven and aft propeller is podded solution. (ABB, 2004; Carlton, 2012 & Molland, 2011)



Figure 10. Contra-rotating propeller variant with podded propeller (ABB, 2004)

In this solution the propellers are not in the coaxial shaft, but they still rotate in different directions and rudder is not needed.

3.4 Propulsion power

To get the required propulsion power first it is needed to estimate the total calm water resistance of the ship in specified speed. The resistance is estimated with scaling model test results in full scale and calculating the resistance factors. The calculation process is described in the Figure 11.

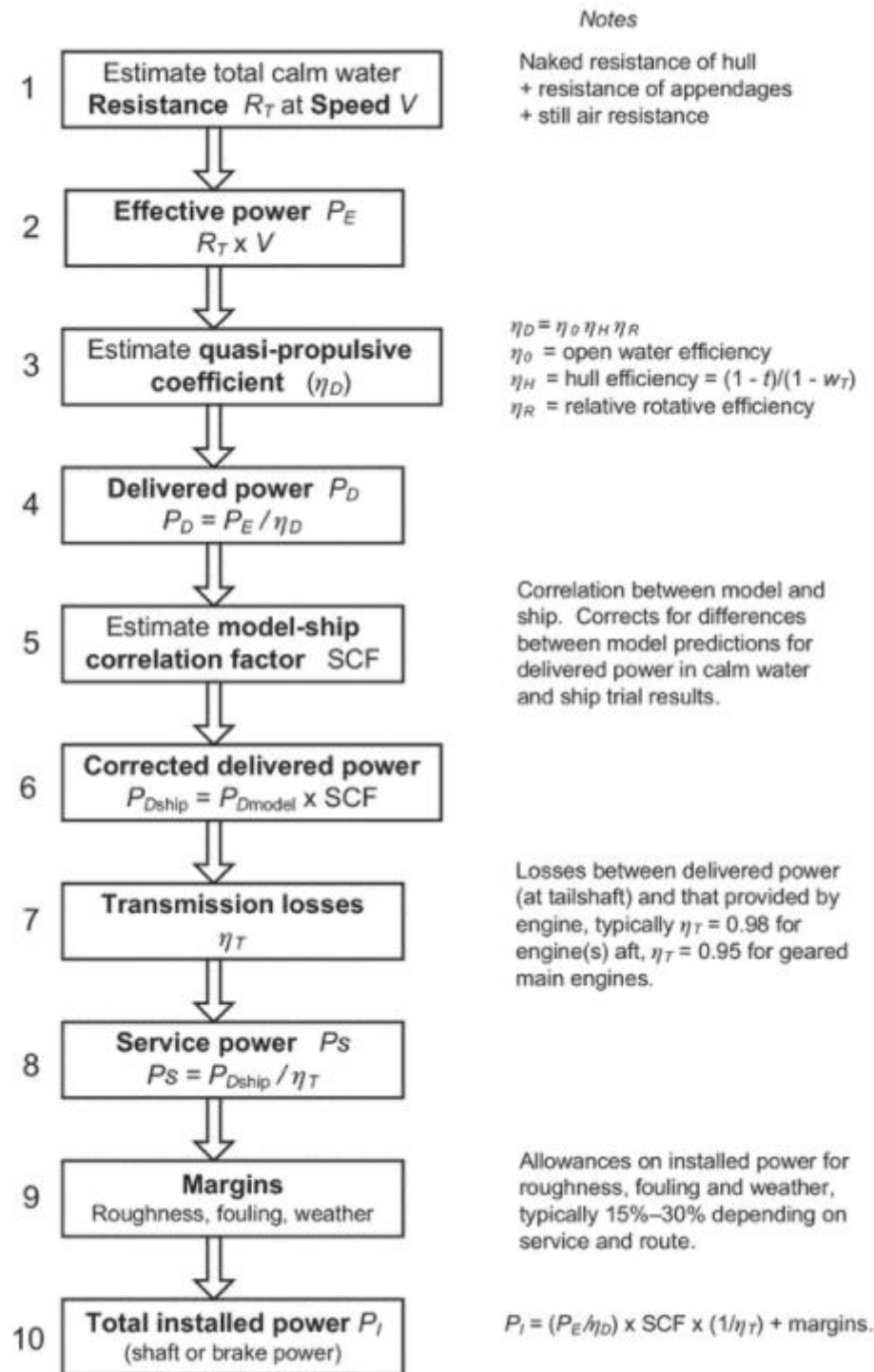


Figure 11. The calculation process to get the total installed shaft power (Molland, 2011)

The model-ship correlation factor and corrected delivered power which are introduced in the steps 5 and 6 are skipped since there are no measurements beyond the model tests available. The total calm water resistance can be divided into three factors which are frictional resistance, residual resistance and air resistance. From the ship total resistance, the frictional resistance is the largest and it depends on the size of the wetted surface area. For low-speed

ships with large wetted surface area it can be from 70 % to 90 % but for high-speed ships it is closer to 40 %. The residual resistance is estimated to be 10-25 % in low-speed ships and from 40 % up to 60 % in high-speed ships. (Wärtsilä, n.d. c)

Marintek has made model tests for similar hull form as the ship in this study has. The model has been named as M2375J (Marintek, 2004). The hull model data can be scaled to full scale ship assuming that the model ship and ship in this study is geometrically similar. The scale factor λ can be calculated with equation

$$\lambda = \frac{L_s}{L_m} = \frac{142 \text{ m}}{5.453 \text{ m}} = 26.04 \quad (1)$$

where L_s represents length of the ship and L_m is the length of the model ship. In this case the model scale is approximately 1:26. Scaling results and model ship hull data is shown in Table 1.

Table 1. Model ship M2375J hull data scaled to full scale RoPax ferry (Marintek, 2004)

		Unit	Ship	Model
Length overall	L_{OA}	m	142.000	5.453
Length on designed waterline	L_{WL}	m	136.505	5.242
Length between perp.	L_{PP}	m	133.172	5.114
Breadth moulded	B	m	23.020	0.884
Draught at LPP/2	T	m	6.588	0.253
Draught at FP	T_{FP}	m	6.588	0.253
Draught at AP	T_{AP}	m	6.588	0.253
Trim (pos. aft)	t	m	0.000	0.000
Volume displacement	∇	m ³	11566.443	0.655
Displacement	Δ	t	11566.443	0.655
Block coefficient	C_B	-	0.5552	0.5727
Wetted surface	S	m ²	3935.801	5.804
Wetted surface of transom stern	A_T	m ²	10.850	0.016
Projected area of the ship above the water line to the transverse plane	A_{vs}	m ²	278.13	-

The total resistance coefficient of the ship is calculated with equation

$$C_T = C_F + \Delta C_F + C_A + C_W + C_{AA} \quad (2)$$

where C_F is frictional resistance coefficient, ΔC_F is roughness allowance, C_A is correlation allowance, C_W is wave resistance coefficient and C_{AA} is air resistance coefficient. From these the wave resistance coefficient represents the residual resistance part of the total resistance. (ITTC, 2008)

The frictional resistant coefficient is calculated with equation

$$C_F = \frac{0.075}{(\log R_e - 2)^2} \quad (3)$$

where the R_e is the Reynolds number (ITTC, 2011 a). The frictional resistance follows the Reynolds number which can be calculated with equation

$$R_e = \frac{L_{pp} \cdot v_s}{\nu} \quad (4)$$

where L_{pp} is the length between perpendiculars, v_s is the speed of the ship and ν is the viscosity of water (ITTC, 2011 a). Roughness allowance also follows the Reynolds number as shown in equation

$$\Delta C_F = 0.044 \left[\left(\frac{k}{L_{WL}} \right)^{\frac{1}{3}} - 10 \cdot R_e^{-\frac{1}{3}} \right] + 0.000125 \quad (5)$$

where k is the roughness of the hull surface, L_{WL} is the length on the designed waterline. The standard value for roughness of the hull k is $150 \cdot 10^{-6}$. (ITTC, 2008)

The correlation allowance is calculated with equation

$$C_A = (5.68 - 0.6 \cdot \log R_e) \cdot 10^{-3} \quad (6)$$

The correlation allowance comes from the comparison of the model and full-scale ship trial results where ITTC recommends using the equation 6 (ITTC, 2008). Air resistance coefficient is calculated with equation

$$C_{AA} = C_{DA} \frac{\rho_A \cdot A_{vs}}{\rho_W \cdot S} \quad (7)$$

where C_{DA} is the air drag coefficient, ρ_A is the density of air, A_{vs} is the projected area of the ship above the waterline to the transverse plane, ρ_w is the density of water and S is the wetted surface of the ship. The air drag coefficient can be determined by wind tunnel model, tests or calculations which typically fall in range of 0.5 to 1.0 where the typical default value is 0.8 which is also used in this calculation. (ITTC, 2008)

The wave resistant coefficient is normally calculated using the subtraction of the total resistance and frictional resistance. Since there are no test results and measured data this leaves us with two variables in the equation. However, to get the close enough prediction of the wave resistance coefficient, the given estimation range of 10 % to 25 % for low-speed ship and 40 % to 60 % for high-speed ship can be used. Since the designed speed 21 knots is not high-speed nor low-speed ship, we can estimate the share of the wave resistance coefficient to be 30 % of the total resistance coefficient.

The seawater temperature change during year in the front of the Helsinki sea area is shown in Figure 12.

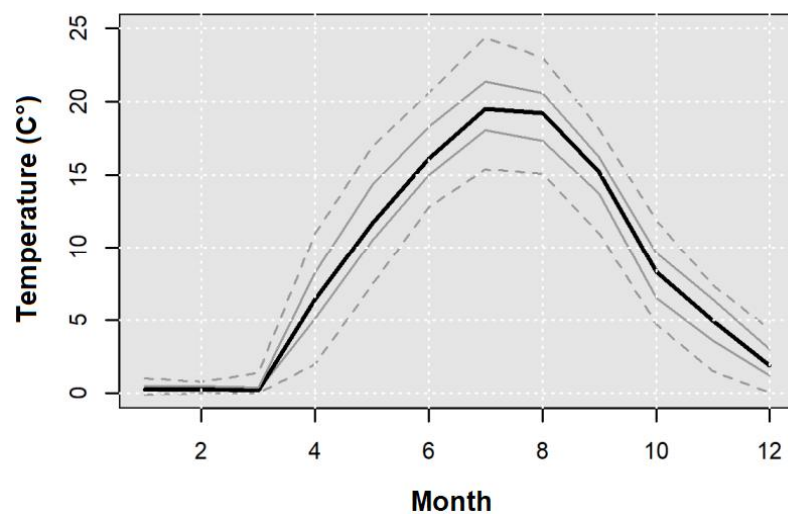


Figure 12. Seawater temperature in front of the Helsinki sea area in under 6m depth (Helsinki, 2018)

From the graph the average seawater temperature during the whole year is approximately 7 degrees Celsius. With this temperature the seawater density and kinematic viscosity can be defined from Figure 13.

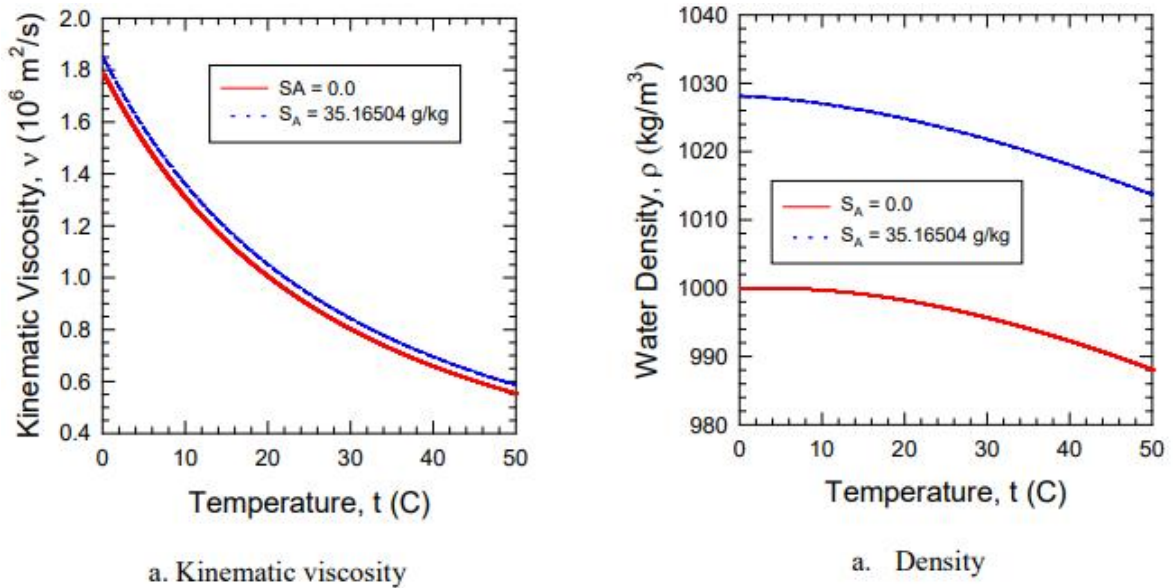


Figure 13. Kinematic viscosity and density of water depending of temperature (ITTC, 2011 b)

For the density of air, the used value is 1.255 kg/m^3 in the temperature of 8 degrees Celsius which was the average air temperature between 2019 and 2020 in Helsinki (Ilmatieteenlaitos, 2020). Kinematic viscosity and water density are received from the Figure 13 in average water temperature of 7 degrees Celsius. Table 2 shows the values received from the Figures 12 and 13. The blue line with approximately 35.17 g/kg mean absolute salinity is used since it is the average absolute salinity value.

Table 2. Properties of the air and water

Air density in 8 C°	ρ_A	kg/m^3	1.255
Density of water in 7 C°	ρ_W	kg/m^3	1027.5
Viscosity of water in 7 C°	ν	m^2/s	$1.48\text{E}-06$

Since this study does not focus on the hydrodynamics, some shortcuts in the calculations are made to simplify the process. As the wave resistance coefficient is estimated to be 0.3 times total resistance, the equation 2 can be redefined as

$$\begin{aligned}
C_T &= C_F + \Delta C_F + C_A + 0.3 \cdot C_T + C_{AA} \rightarrow \\
C_T - 0.3 \cdot C_T &= C_F + \Delta C_F + C_A + C_{AA} \rightarrow \\
0.7 \cdot C_T &= C_F + \Delta C_F + C_A + C_{AA} \rightarrow \\
C_T &= \frac{1}{0.7} \cdot (C_F + \Delta C_F + C_A + C_{AA}) \rightarrow
\end{aligned}$$

Now the equations 3-7, the values from Table 1 and Table 2 can be placed in the modified equation 2

$$\begin{aligned}
C_T &= \frac{1}{0.7} \cdot \left(\frac{0.075}{\left(\log \left(\frac{133.172 \text{ m} \cdot (21 \cdot 0.5144) \frac{\text{m}}{\text{s}}}{1.48 \cdot 10^{-6} \frac{\text{m}^2}{\text{s}}} \right) - 2 \right)^2} \right. \\
&\quad + 0.044 \left[\left(\frac{150 \cdot 10^{-6}}{136.505 \text{ m}} \right)^{\frac{1}{3}} - 10 \cdot \left(\frac{133.172 \text{ m} \cdot (21 \cdot 0.5144) \frac{\text{m}}{\text{s}}}{1.48 \cdot 10^{-6} \frac{\text{m}^2}{\text{s}}} \right)^{-\frac{1}{3}} \right] \\
&\quad + 0.000125 + \left(5.68 - 0.6 \cdot \log \frac{133.172 \text{ m} \cdot (21 \cdot 0.5144) \frac{\text{m}}{\text{s}}}{1.48 \cdot 10^{-6} \frac{\text{m}^2}{\text{s}}} \right) \cdot 10^{-3} \\
&\quad \left. + 0.8 \frac{1.255 \frac{\text{kg}}{\text{m}^3} \cdot 278.13 \text{ m}^3}{1027.5 \frac{\text{kg}}{\text{m}^3} \cdot 3935.8 \text{ m}^2} \right) = 2.90 \cdot 10^{-3}
\end{aligned}$$

The effective power can be calculated with equation

$$\begin{aligned}
P_E &= C_T \cdot \frac{1}{2} \cdot \rho_w \cdot v_s^3 \cdot S_s & (8) \\
&= 2.90 \cdot 10^{-3} \cdot \frac{1}{2} \cdot 1027.5 \frac{\text{kg}}{\text{m}^3} \cdot \left((21 \cdot 0.5144) \frac{\text{m}}{\text{s}} \right)^3 \\
&\quad \cdot 3935.8 \text{ m}^2 = 7323.93 \text{ kW}
\end{aligned}$$

Effective power represents the power that is required to tow the ship. The propeller properties are not taken account in this power. These calculations can be repeated for the speed range and above to get the effective power dependence from the speed (Figure 14).

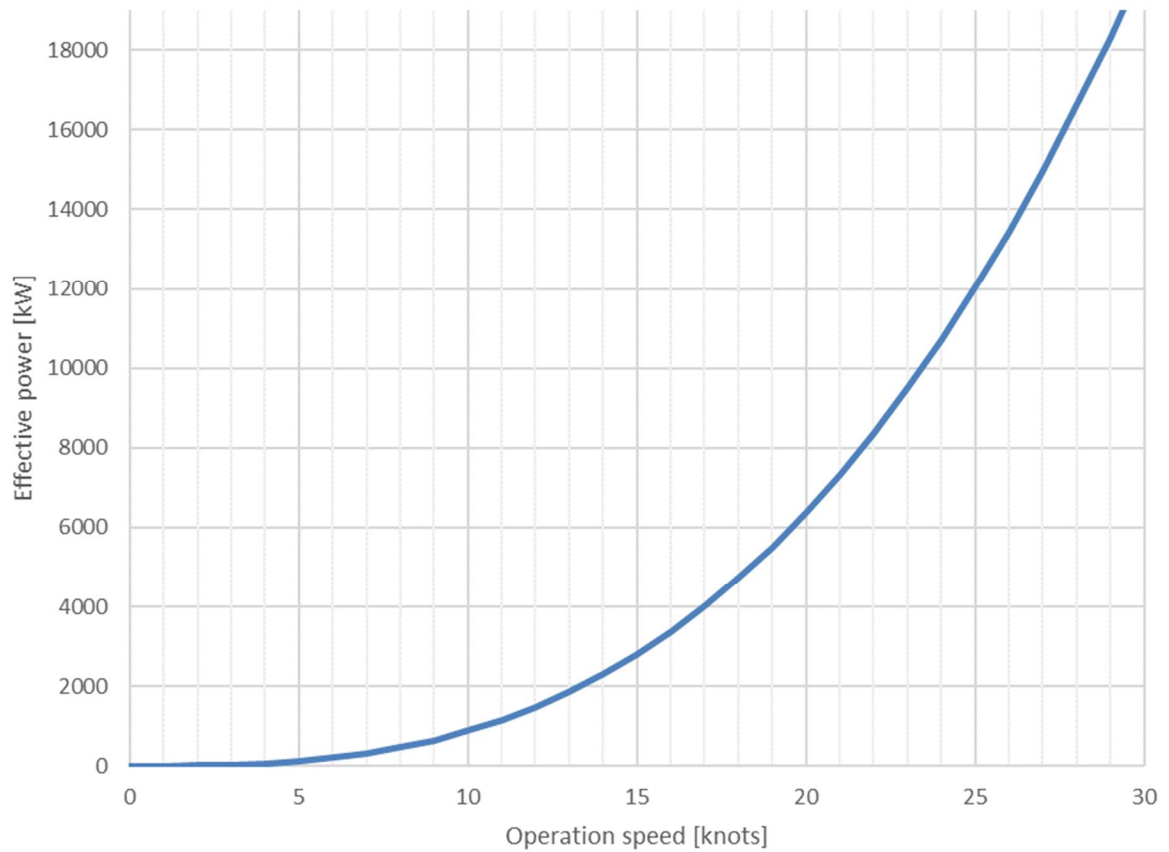


Figure 14. Effective power depending on the operating speed

Step 3 in Figure 11 is to estimate the Quasi-Propulsive Coefficient (QPC) and then the effective power is divided with it to get the delivered power. The QPC represents the propulsive efficiency and in other words the losses on propeller at the shaft output. Usually, the QPC falls in range of 0.55 to 0.65. (Marineinsight, 2019)

In these calculations the QPC of 0.55 is used. The delivered power is calculated with equation

$$P_D = \frac{P_E}{QPC} = \frac{7323.93 \text{ kW}}{0.55} = 13316.23 \text{ kW} \quad (9)$$

The delivered power represents the power that the shaft delivers to the propeller. To get the service power that the main engine and generator set generates the transmission losses needs to be taken into account. The transmission efficiency η_T of 0.95 which is get from the Figure 11 is used. The service power is calculated with equation

$$P_S = \frac{P_D}{\eta_T} = \frac{13316.23 \text{ kW}}{0.95} = 14017.08 \text{ kW} \quad (10)$$

Since the operation conditions vary from day to day there is need for sea margin to get the total installed power. In Figure 11 the recommended sea margin is between 15 to 30 percent depending on the operation route. Since the operating route is relatively easy operated the sea margin is decided to be 15 percent. Total installed power is then calculated with equation

$$P_T = \frac{P_S}{1 - k_{sm}} = \frac{14017.08 \text{ kW}}{1 - 0.15} \approx 16120 \text{ kW} \quad (11)$$

The generators need to be able to feed 16120 kW to the propellers to be able to operate in 21 knots operating speed. The propulsion powers follow the Figure 14 values. Acceleration forces are mainly neglected in this study since the evaluation process demands more characteristic data that is not available although it has an effect to the result. For more detail analysis the acceleration forces are needed to take into account.

3.5 Electrical energy consumption

The electrical energy consumption in ferry operation consists mainly of ship propulsion. The propulsion set is defined to be 8.1 MW each with total propulsion power of 16.2 MW. Hotel load in its maximal load is 1.1 MW but the use of the electrical consumers is not simultaneous. There are two thrusters with 700 kW each and total of 1400 kW. The deck machinery units such as mooring equipment and winches are used in ports mainly. Lightings are possibly used more at ports since the docking area might sometimes be dark and additional deck lights might be needed to dock. Navigation equipment is used mainly in sea operation. Air conditioning and kitchen electrical loads are quite stable but in port the power requirement is not as much as in the sea operation. Auxiliary machinery units are used quite stable all the

time. With these assumptions the electrical loads for the single day operation are presented in the Figure 15.

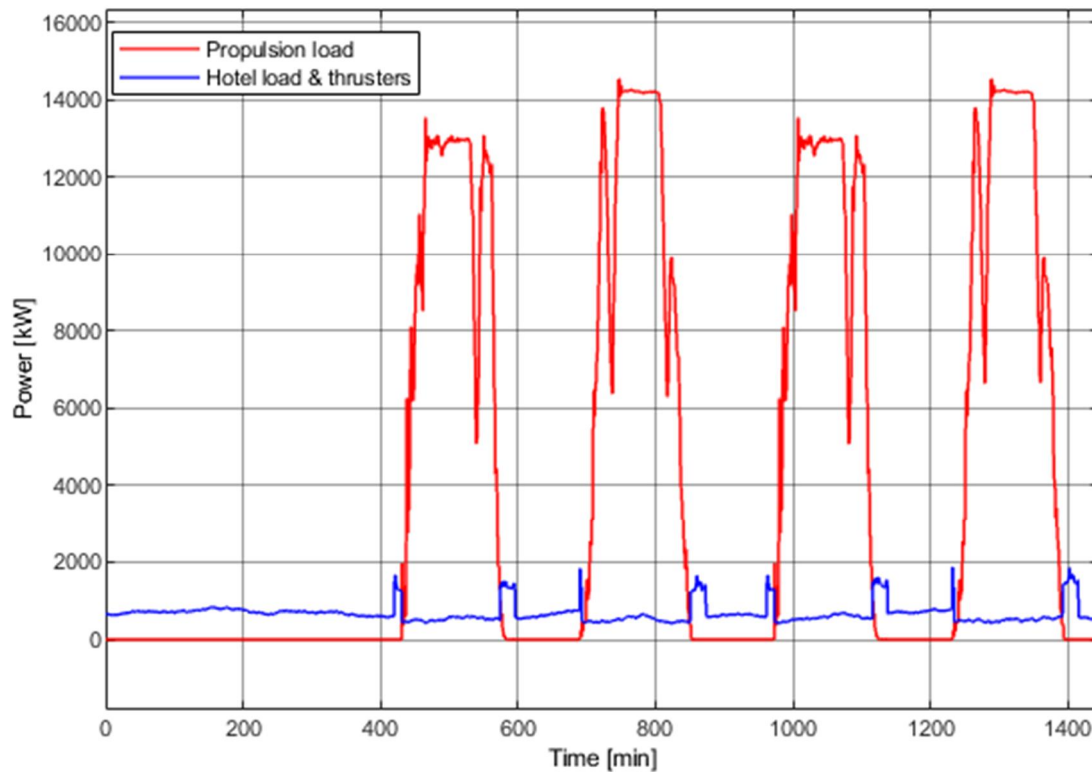


Figure 15. Electrical loads in single day operation

The load cycling comes from the assumption that the ship makes two back and forth trips a day and is docked for night. The propulsion load peaks at slightly over 14 MW. The reason for the higher peak propulsion loads in the other way is that the operating conditions, wind and waves demand higher power to be able to manoeuvre in designed operation speed. The power drops to approximate 6 MW from the peak when the ship is in the point of route where the fairway turns significantly, and the speed is decreased when large steering movement is needed. The average hotel load is approximately 600 kW. The tunnel thruster loads are added to the hotel load since same generators serve them. The peak power is approximately 15 MW and the total electrical energy consumption is 117.5 MWh. The load distribution is presented in Figure 16.

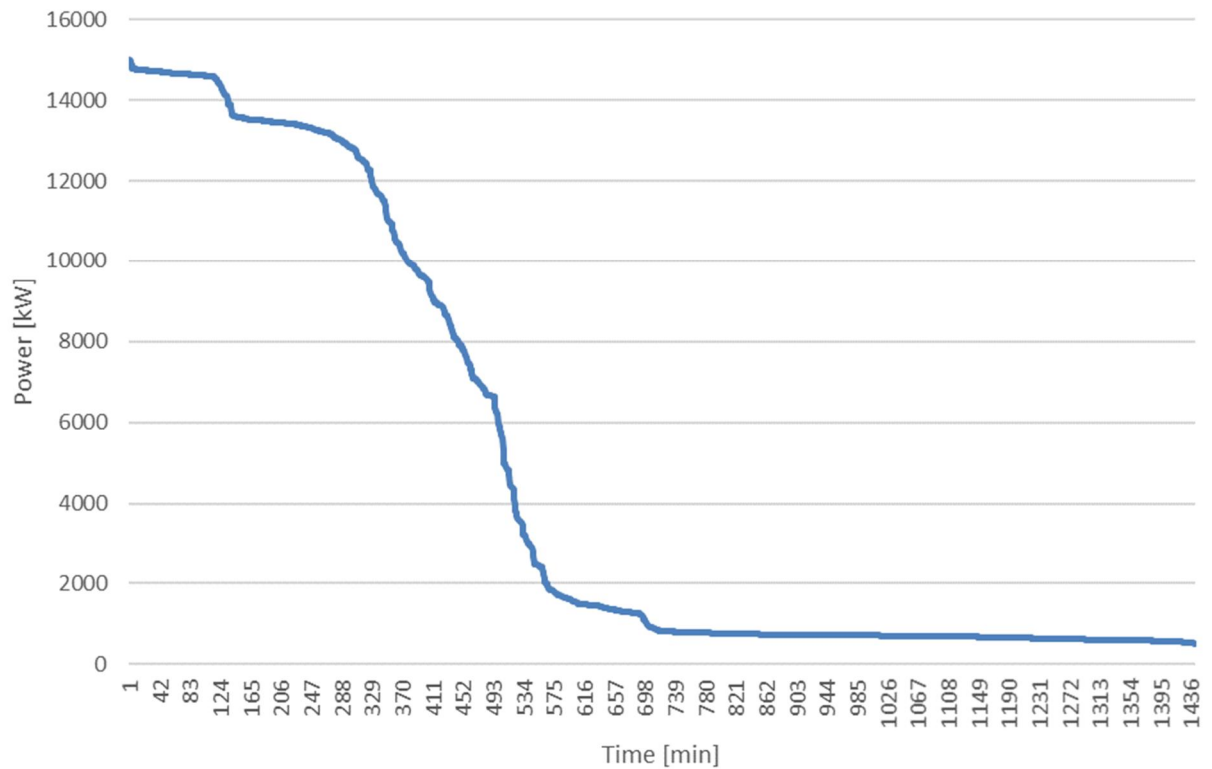


Figure 16. Load duration distribution

Over half a time the load is under 1 MW which indicates that the ship is docked in port total of half a day.

3.6 Main engines and generator sets

Main engines turn fuel into mechanical rotation movement which is then used to rotate the generator to generate electricity. Rules and regulations set the requirement for the main engine selection so that they meet the load demands in the designed operational conditions. (Bureau Veritas, 2018 & DNV GL, 2019a)

Propulsion power demand was 8.1 MW for each propeller with total of 16.2 MW power demand to reach the designed speed. Propellers are shaft driven so for each shaft the main engines need to provide the 8.1 MW power. The main engines that power the propulsion the selection is Wärtsilä 16V31 for each shaft with engine output being 9440 kW and generator output being 9060 kW (Wärtsilä, 2020).

Thrusters get the feeding from the same generators than hotel load which is maximum of 1100 kW. The total requirement for the hotel load generators is at least 2500 kW. The main engine selection is two Wärtsilä 8L20 with 1480 kW engine output and with the generator output power of 1405 kW each. The engine is not recommended to run in under 30 % loading for a long time since it affects the engine unit negatively and causes engine wet stacking where there are oil leaks caused by the underloading. The continuous operating field of W31 engine is shown in Figure 17 (CAT, 2013 & Wärtsilä, 2020)

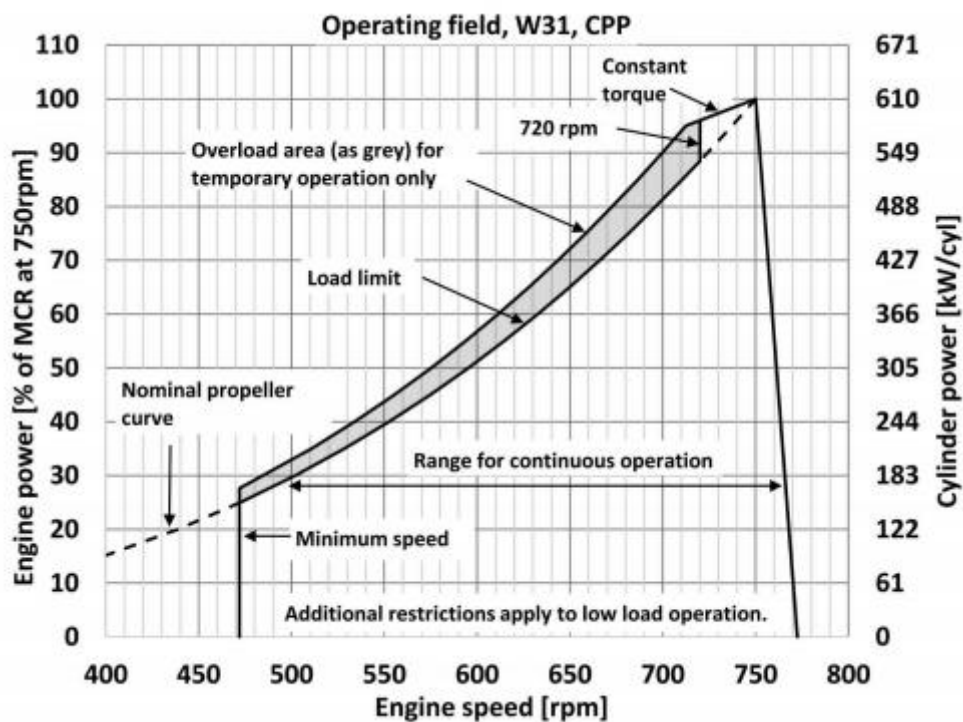


Figure 17. Operating field of Wärtsilä 31 engine (Wärtsilä, 2020)

The minimum loading for continuous operation is approximately 30 %. In the propulsion load curve in Figure 15 divided for the two engines there are quite long periods of underloading if driven in load following mode. Even though the engine is capable of handling low loads shown in propulsion load curve, the engine is driven with minimum loading of 30%.

In the start-up the engine can reach 100 % loading in 80 seconds with normal operating temperature according to Figure 18.

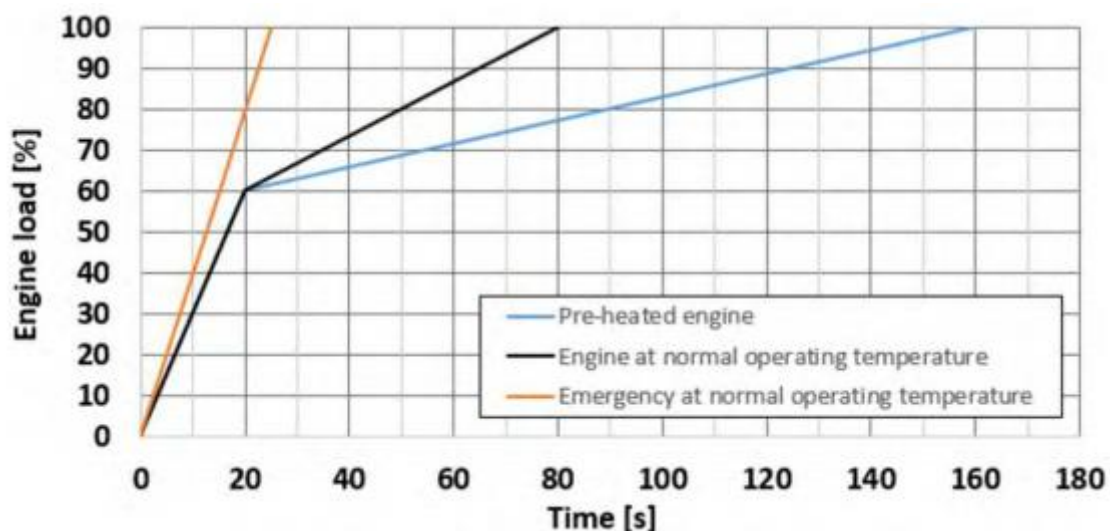


Figure 18. Maximum recommended load increases in nominal operation speed (Wärtsilä, 2020)

The 30 % loading is reached in 10 seconds in any conditions, so the variation of the load increasing is not seen in the graphs on this study since the time interval is 1 minute.

Additional to these there is also emergency generator needed which is excluded from this study since the energy storage dimensioning analysis does not require to take emergency conditions into account. Emergency generator is not used to load the energy storage, but the excessive energy can be used in emergency conditions. However, these conditions are neglected in this study. The base values are now decided so that the ship main components and operation values are shown in Table 3.

Table 3. Base values and main components of the ship

One-way trip length	81.7 km
Number of one-way trips	4
Size of the ship	16 000 GT
Length of the ship	142 m
Propeller nominal load	2 x 8100 kW
Tunnel thruster nominal load	2 x 700 kW
Main engine 1&2 nominal power	2 x 9440 kW
Generator 1&2 nominal power	2 x 9060 kW
Main engine 3&4 nominal power	2 x 1480 kW
Generator 3&4 nominal power	2 x 1405 kW
Maximum hotel load without thrusters	1100 kW

4. ELECTRICAL ENERGY STORAGE

As mentioned in marine applications the main source of energy is the main engines and generator set which converts fuels to electrical energy. The energy storage main purpose is to store excessive energy for later use. It can for example be used to improve energy efficiency or to use it as power reserve. (Komarnicki, 2017)

4.1 Energy storage options

There are many different options to store energy (Figure 19). For high power and high capacity uses there is pumped hydro- and compressed air energy storage. These two are used in the bulk power management where in the larger scale the peak shaving or power reserve is needed and reserves a lot of space which is not available in ships.

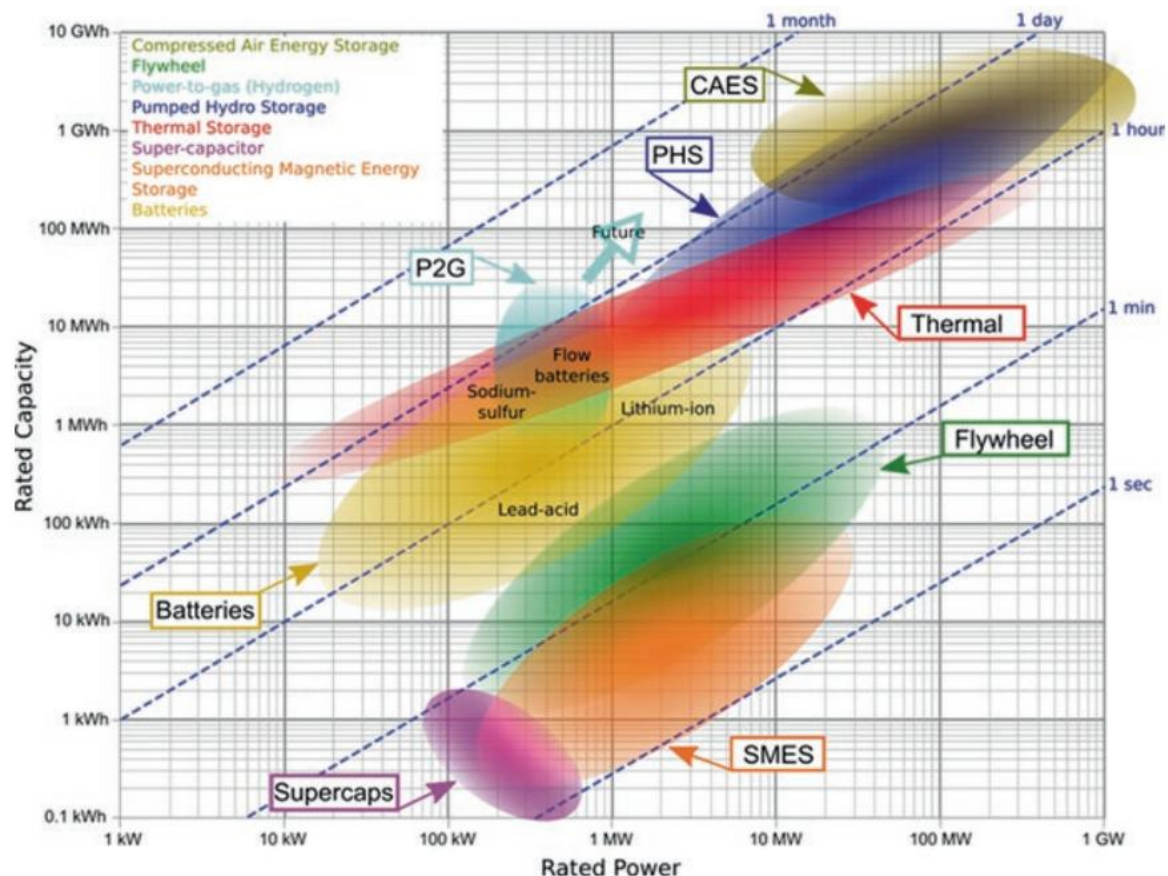


Figure 19. Energy storage applications (Komarnicki, 2017)

Medium power and medium capacity applications are batteries, thermal storages and power to gas. Capacitors, flywheels and superconducting magnetic energy storages represents the low-capacity options.

Thermal storages can be used to recover energy from waste heat in ships. Thermal storages are usually used in industrial and residential sector. However, the heat conversion phase is very slow and therefore not suitable for loads which need high response time. (Ali, 2021)

In power to gas concept the ship would need to have either hydrogen tanked straight to ship or electrolyser to generate it from water. In electrolyser the water and electricity are fed to the system and hydrogen and oxygen is released. In fuel cell the hydrogen and oxygen are fed to the system to generate water and electricity. The cost of these electrolysers can be as high as 1000-2000 €/kW. (Oxford Institute, 2018)

Flywheel energy storage function is based on a kinetic energy stored in a large wheel which stores the energy for a short duration. It can be combined for example with capacitors to store the energy. In ships this can be used in main engine shafts but for a large-scale long duration energy storage it is not suitable. (Olabi, 2021)

The capacitors and superconducting magnetic energy storages are not suitable on its own since the duration is not long enough for these kinds of marine applications but combined with other solution such as batteries the peak powers could be supplied with energy from capacitors and continuous powers from battery packs.

Battery energy storages can have high capacity and power qualities at the same time. Battery energy storages are selected for further analysis in this study.

4.2 Battery materials

There are several different options for battery technology. There is nickel based, lead based and lithium-based chemistries available from which the lithium-based batteries are the most commonly used in these kinds of purposes. Compared to nickel and lead based battery technologies the lithium batteries have higher voltage and energy density and also lower rate of self-discharge. Therefore, the capacity loss over time is less than with other technologies. The capacity loss is in some cases permanent and in some cases reversible where the capacity is regained when battery is cycled. Lithium-ion technologies also have much better cycle life than other battery technologies. That is why the more detailed analysis is focused on lithium-based battery technologies. (Warner, 2015)

Lithium-ion cells consists of electrodes which are anode and cathode, electrolyte and external circuit. It depends on the used technology that is the electrodes and electrolyte solid or liquid material but either way they are in contact with each other. The basic principle is that when charging the battery, anode gives positive ions to electrolyte and oxidizing and charging itself with electrons. Cathode receive electrons through external circuit while reducing itself. Cathode receives positive ions through from the electrolyte and gives negative ions to the electrolyte. This redox reaction happens for both the positive and negative electrodes (Figure 20). (Komarnicki, 2017 & Santhanagopalan, 2015)

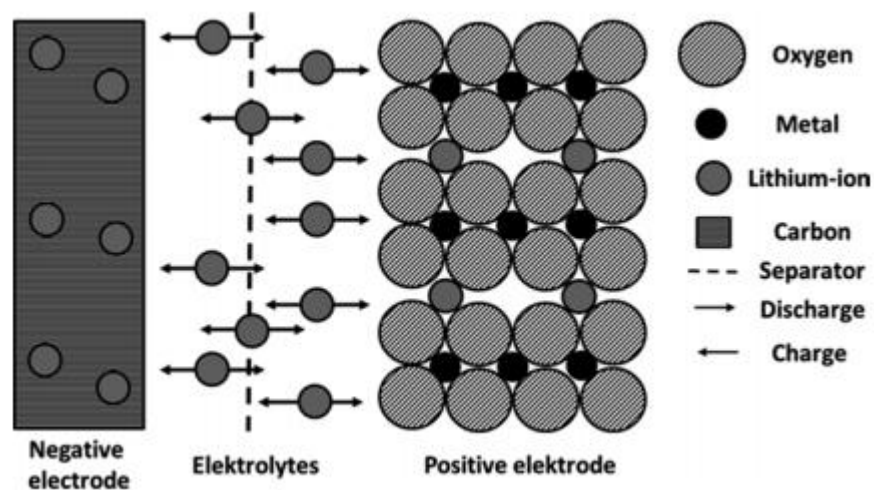


Figure 20. Charging and discharging principle of lithium-ion cells (Komarnicki, 2017)

There are three categories of lithium-ion battery cathodes. They are layered transition-metal oxides, spinels and olivines (Figure 21). Layered oxides have typically highest capacity but also the cost of the cell rises at the same time and cell safety decreases. Spinel has very high power density and lower cost of cell but does have also safety concerns which are based on structural stability and poor electronic conductivity. (Santhanagopalan, 2015)

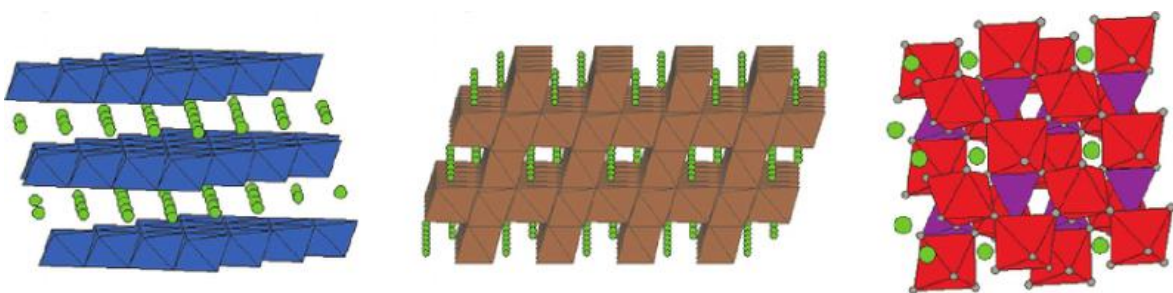


Figure 21. Layered oxide, spinel and olivine structures respectively (Camilo, 2006)

The very first layered oxide was a lithium cobalt oxide but later on the cost and toxic content of cobalt forced to develop alternatives with lower cobalt contents such as lithium nickel cobalt aluminium oxide (NCA) and lithium nickel manganese cobalt oxide (NMC). With the reduced costs these two also has a higher energy content, power delivery and lifespan than earlier version with cobalt only. (Santhanagopalan, 2015)

Spinel structure liberates lower amount of oxygen and heat in extreme condition operation. Therefore, the spinel structure has an improved safety. Spinel is typically in lithium manganese oxide in which the manganese is cheaper than cobalt or nickel or lithium titanate oxide (LTO). However, the lithium manganese oxide is loss relevant option for battery selection nowadays. Lithium titanate oxide is also in spinal structure. It is said to be one of the safest lithium-ion batteries available. Spinal structure allows higher power and efficiency, but the downside is lower specific capacity. (Batteryuniversity, 2019 & Santhanagopalan, 2015)

From olivines the most typical is lithium iron phosphate (LFP) which is also one of the safest lithium-ion batteries. The stability of the structure allows excellent cycle life for the batteries. However, the specific energy and cell voltage suffer from the lithium holding capacity. (Santhanagopalan, 2015)

4.2.1 Lithium Nickel Cobalt Aluminium Oxide

NCA battery is a layered metal oxide structured battery and uses nickel cobalt aluminium as its cathode and graphite as anode. Aluminium increases the thermal stability and electrochemical performance in NCA but still it is not as safe as other lithium batteries and thermal runaway happens in 150 degrees Celsius. NCA offers a high specific energy solution as seen in Figure 22. (Batteryuniversity, 2019 & Berg, 2015)

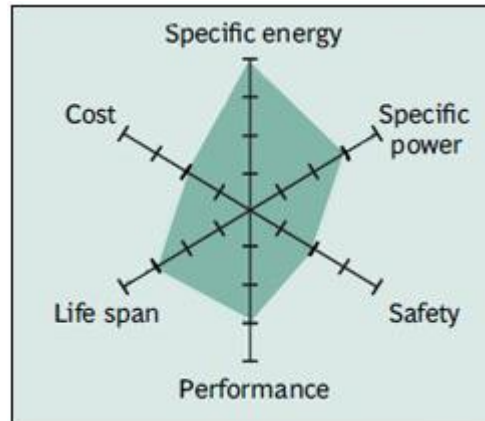


Figure 22. NCA battery characteristics (batteryuniversity, 2019)

The cycle life of NCA is quite poor compared to other lithium batteries with only 500 cycles depending on the depth of discharge (DoD) and temperature. However, the specific energy is from 200 to 260 Wh/kg which is the best of the alternatives compared in this study. The cost of cell is quite cheap with 290 €/kWh in 2019. (batteryuniversity, 2019)

4.2.2 Lithium Nickel Manganese Cobalt Oxide

Lithium nickel manganese cobalt oxide (NMC) is Lithium-ion battery technology which uses nickel, manganese and cobalt as its cathode and graphite as anode. It is also layered metal oxide structured as NCA. Compared to NCA the aluminium is replaced with manganese. Nickel has a high specific energy but a poor stability while manganese forms the spinel structure which offers low internal resistance with low losses but low specific energy. With these two combined they enhance each other. NMC characteristics are shown in Figure 23. (batteryuniversity, 2019)

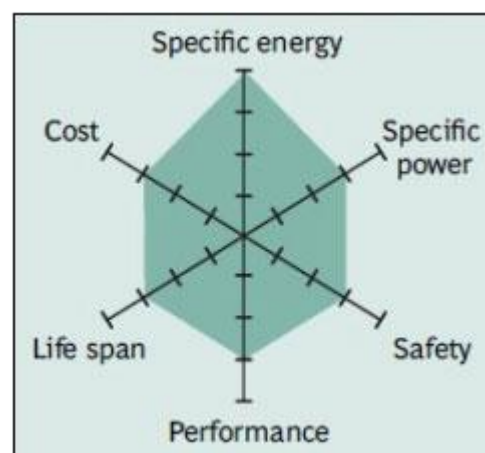


Figure 23. NMC battery characteristics (batteryuniversity, 2019)

NMC is quite balanced lithium battery with good cycle life of 1000-2000 cycles and very good specific energy of 150-220 Wh/kg. However, it is lower specific energy than with NCA because of the manganese. C-rates are usually around 1C and cell cost approximately 350 €/kWh in 2019. (batteryuniversity, 2019)

4.2.3 Lithium Iron Phosphate

LFP has olivine structure where in the cathode the Lithium and Iron is in octahedral sites and Phosphorus in tetrahedral sites in a distorted hexagonal closed oxygen array. Graphite is used as anode. The capacity of LFP is medium, usually from 90 to 120 Wh/kg. The rate capability is Utilizing the nano particles will increase the electronic conductivity for a short diffusion times which allows short time C-rates to be as high as 25. The characteristics of LFP is shown in Figure 24. (Batteryuniversity, 2019 & Berg, 2015)

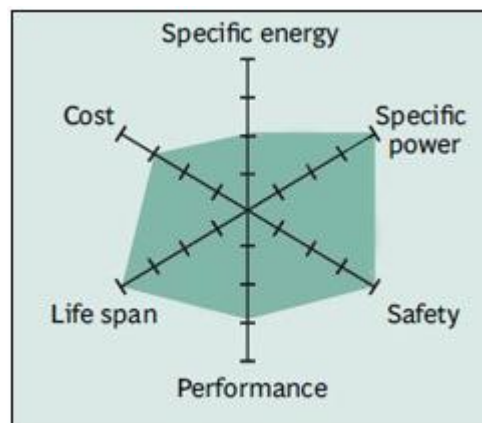


Figure 24. Lithium iron phosphate -battery characteristics (batteryuniversity, 2019)

Thermal stability for the charge and discharge state is high. In low temperatures as in the most batteries the performance is reduced. LFP has a higher self-discharge than other lithium batteries. However, with good control electronics this is not an issue. LFP needs a clean space for operation and has no tolerance for moisture. The usual cycle life is around 2000 cycles, but it also can be much higher even to 4000 cycles as seen in Figure 25. The usual cell price is 490 €/kWh in 2019. (Batteryuniversity, 2019 & Berg, 2015)

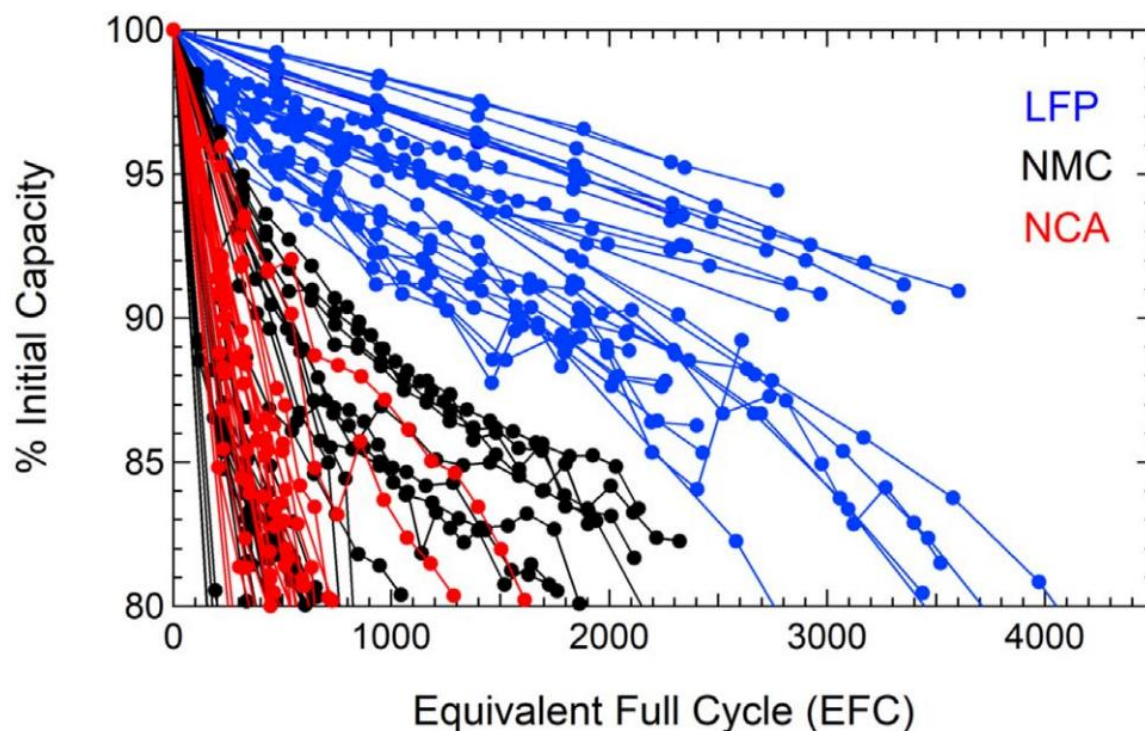


Figure 25. Cycle life of LFP, NMC and NCA cell technologies compared (Preger, 2020)

The cycle life of LFP can be considered as 2000 to 4000 cycles which makes LFP a very good option for energy storage.

4.2.4 Lithium Titanate

LTO has a spinel structure and it replaces the graphite with titanate in its anode. The cathode material could be for example manganese oxide or NMC. LTO has a very good thermal stability, high C-rates and high cycle life. The downside of the LTO is that the cost of titanium is high which rises the cell prices and the cell voltage and capacity is lower than in other types of lithium batteries. LTO has these good characteristics because of very low probability of phase change during lithiation or delithiation. The anodes in LTO batteries can last even tens of thousands of cycles, but usually the cycle life is around 3000 to 7000 so either way LTO is very long-lasting choice. These characteristics makes LTO a good option for a high power, high cycle life but low energy option (Figure 26). (Batteryuniversity, 2019 & Nitta, 2015)

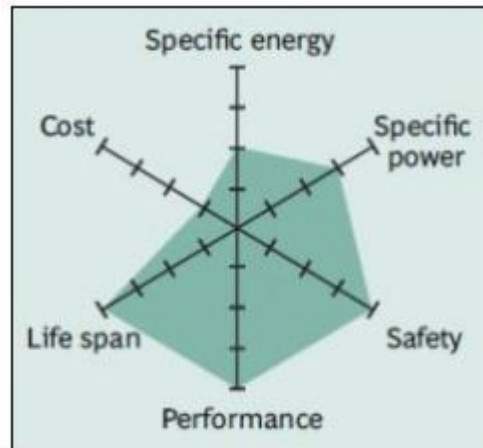


Figure 26. Lithium titanate -battery characteristics (batteryuniversity, 2019)

The C-rates of LTO are very high while it is capable of charging with 1-5C and discharging with continuous 10C. It is one of the safest lithium batteries available. LTO has also good low temperature characteristics as it can operate in -30 Celsius degree temperature with 80 % capacity. The specific energy of the LTO is only from 50 to 80 Wh/kg which means that quite large system is needed compared to other lithium batteries. Weight is a crucial part in shipbuilding technology so that is one issue. In addition, the cell price is over 840 €/kWh in 2019, so the technology is also very expensive compared to other lithium batteries. (batteryuniversity, 2019)

4.3 Comparison of lithium batteries

All of these previous mentioned lithium battery type characteristics are listed in Table 4 for comparison.

Table 4. Lithium battery cell characteristics (batteryuniversity, 2019.; Pareger, 2020 & Warner, 2015^(*))

	NCA	NMC	LFP	LTO
Voltage range [V]	3.0-4.2	3.0-4.2	2.5-3.65	1.8-2.85
Specific energy [Wh/kg]	200-300	150-220	90-120	50-80
Volumetric density [Wh/L] ^(*)	210-600	325	220-250	130
Charge C-rate	0.7	0.7-1	1	1-5
Discharge C-rate (short time)	1	1 (2)	1 (25)	10 (30)
Cycle life	500	1000-2000	2000-4000	3000-7000
Cost of cell [€/kWh]	290	350	490	840
Thermal runaway [°C]	150	210	270	-

LTO is one of the safest batteries with good thermal stability. Thermal runaway depends on the cathode material. LTO has also the lowest cell voltage levels. In shipbuilding the mass and volumes of the material are crucial values and if there would be installation of a battery packs it would be best to get as much capacity as possible in as little space as possible. The best specific energies are in NCA and NMC batteries. The cycle life and cost of cells are also very important factors since the system cannot cost too much to be useful and should last as long as possible also that it is not needed to replace often.

4.4 Control methods

Battery management system (BMS) ensures the safe operation with energy storages. BMS collects measured information from the cells and controls the operation. The usual measured values in whole energy storage scale are the battery SOC, state of health, charge and discharge limits. In smaller scale there are measured cell and pack voltages, temperatures, powers and currents. BMS also controls the auxiliary systems such as cooling fans and pumps and other connected devices. (Weicker, 2014)

In marine operations since the Power management system (PMS) also controls the whole ship power generation and distribution the BMS is needed to be connected to it. BMS shares the measured values and PMS controls the operation so that the generators are controlled based on the SOC of the energy storage. PMS uses previous trend curve and history data to estimate the daily electric consumption and controls the limited power which of course could vary from day to day. Figure 27 presents the basic principle of BMS operation in ship.

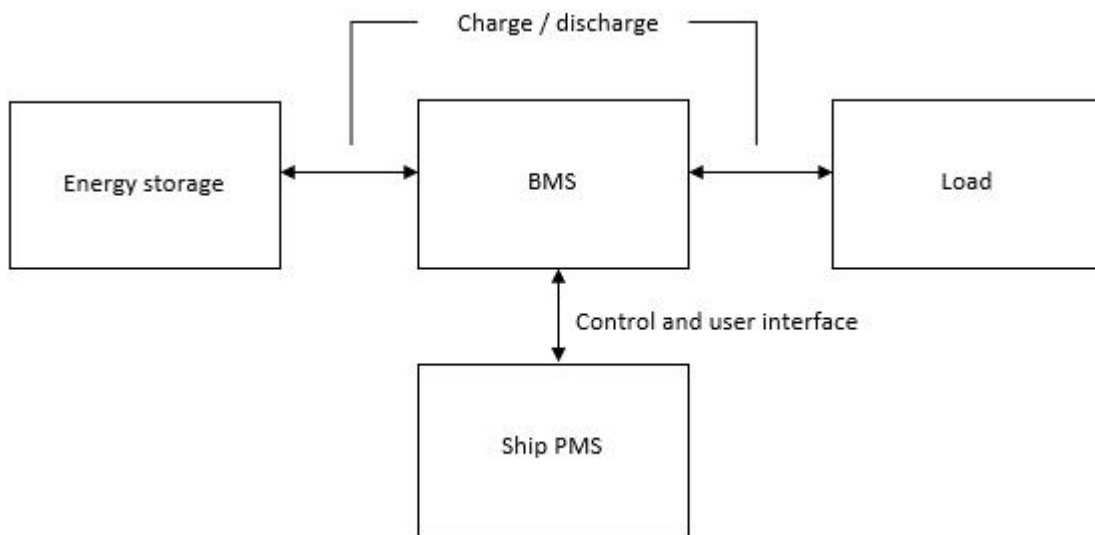


Figure 27. Battery management system block diagram

BMS operates and monitors together with PMS switchgears which either discharges the battery to load or charges it. With high-power applications such as this there can be very high inrush currents which require a lot from safety gears.

Usually the low-power or sleep mode is used which means that the battery is disconnected from the load with opening the contacts. Monitoring is not needed in low-power mode. If the usage of batteries is infrequent it is good to wake up the system periodically to estimate SOC and cell balance more accurately since the cell dynamics relaxes. Cell balancing is also an important function of BMS since the cell charges get unbalanced over time caused by internal leakage which results in capacity drop since the system would charge till the cell is full and discharge till it is empty. If one cell has a higher charge than the other the charging would stop when the higher charge cell is full leaving the other partially charged. (Andrea, 2010 & Weicker, 2014)

BMS should detect and prevent hazards as overcharge and discharge, overcurrent, operation outside of temperature range, ground faults and other control signal faults. It is also preferred to use redundant design so that the control unit is duplicated (Weicker, 2014)

4.5 Regulations and classifications

International maritime organization (IMO) has formed international convention for the safety of life at sea (SOLAS) which main purpose is to set minimum standards for the equipment, construction and operation of the ship so that it is safe to use. Classification societies follows the SOLAS with their own regulations. Also, the flag states of ship set their own requirements. (IMO, n.d. b)

There are multiple classification societies. There are for example DNV GL, Bureau Veritas, RINA, Lloyd's register and from those DNV GL and Bureau Veritas regulations is further examined in this chapter from which DNV GL has much more clear regulations available for lithium-ion batteries.

SOLAS does not have rules for battery fire safety so the classification societies have set it to follow the general fire safety regulations. The energy storages above 20 kWh are divided with power and safety qualifiers. The power qualifier means that the energy storage is a powers source for the electrical propulsion or main source of power. The safety qualifier is for peak shaving and load levelling use and when the energy storage is not used as the main source of power. The design of energy storage must be so that single failure in system does not make any main functions unavailable. Energy storage should contain short circuit protection and overcurrent protection with isolation capabilities. Safety issues as gas development, fire, explosion, external risks should be taken into account. (DNV GL, 2019)

4.5.1 Ventilation

Mechanical ventilation is required in energy storage room. The ducting must be independent from other ventilation system unless the energy storage system is installed in enclosed cabinet with integrated off-gas ventilation duct. If there is such integrated duct the supply air can be taken from ventilation which is also serving other spaces. The requirement for air

change is at least two times in an hour. For the off-gas exhaust the fan capacity should be selected so that it is able to change the air six times in an hour. The energy storage room must be positively pressurized compared to the battery cabinets. There is also needed gas detectors in case of explosive or flammable gas concentrations. Energy storage space ambient temperature is monitored with independent sensors from energy storage system. Areas in open deck within 1.5 m of exhaust or inlet openings of energy storage room is classified as extended hazardous area zone 2. (Bureau Veritas, 2021 & DNV GL, 2019)

4.5.2 Fire safety

The fire integrity of two battery rooms must be A-0 and A-60 towards machinery spaces, enclosed cargo areas and embarkation stations. Doors must be alarmed normally closed doors or self-closing doors. (Bureau Veritas, 2021 & DNV GL, 2019)

Combined smoke and heat detection is installed in energy storage rooms with lithium-ion batteries. The fire exhaustion system is needed to be fixed total-flooding and to be compatible with the battery technology and discussed with manufacturer. (Bureau Veritas, 2021 & DNV GL, 2019)

5. DESIGN OF THE BATTERY ENERGY STORAGE SYSTEM

In this study two different approaches for the energy storage design are shown. The best-case scenario for the energy storage addition would be that the energy storage operation enables savings. The energy storage is dimensioned based on the earlier generated loading data and to utilize it with different approaches. The model is built with Matlab Simulink program.

5.1 Energy storage operation possibilities

There are many ways to utilize energy storage. The usual benefits are improved energy efficiency, lower fuel consumption, lower emissions, reliable operation and system flexibility. In smaller ferries that operate in short distances it is possible to dimension energy storage to replace all diesel engines for zero emission operation. This is considered to be fully electric operation. However, in larger scale operations with long distances this is not possible since the powers and energies required are so large that it is not possible with technologies available. Hybrid backup operations are Uninterruptible Power Supply (UPS) and spinning reserve. These operations require also high energy capacity. UPS ensures that in case of blackouts the necessary equipment stay supplied with batteries for example. Spinning reserve can be used to decrease the number of generators running. Peak shaving and load levelling require medium amount of power and energy. In peak shaving the power peaks are supplied with energy storage and it is charged with excessive energy. Generator runs with average load while the operation allows fuel savings and reduced engine running hours. In load levelling the energy storage smoothens the load changes and it is as a part of peak shaving operation. The benefit is for example in Liquid Natural Gas (LNG) operation where the engine reaction time is slower. (ABB, n.d. & Corvus Energy, 2017)

5.2 Propulsion assistant energy storage

In this scenario the energy storage is dimensioned so that the excessive energy from the propulsion generators compared to propulsion load is utilized as charging energy storage. The energy is then used to lower the propulsion peak loads. As generator can be loaded under 30 % short times but the long-term use is minimum of 30 % loading the excessive energy is either needed to feed into the main switchboard to other consumers or charge it to energy

storage. To simplify the dimensioning and power management it is considered that the energy storage is dimensioned for propulsion use only. The excessive energy from the 30 % generator loading and electrical load difference is charged into the energy storage. The limited power of one generator is 5.6 MW in this case so that the energy- and fuel saving are maximized. The power peaks are limited to 5.6 MW so that all the charged energy during the day can be used. The potential charging power and time gives maximum energy available for charging without any additional charging periods. This estimation from the maximum possible energy available is also parameter for the energy storage capacity. The energy storage capacity is dimensioned so that the excessive energy can be utilized. The propulsion load, propulsion generator generated power and limited generation is shown in Figure 28.

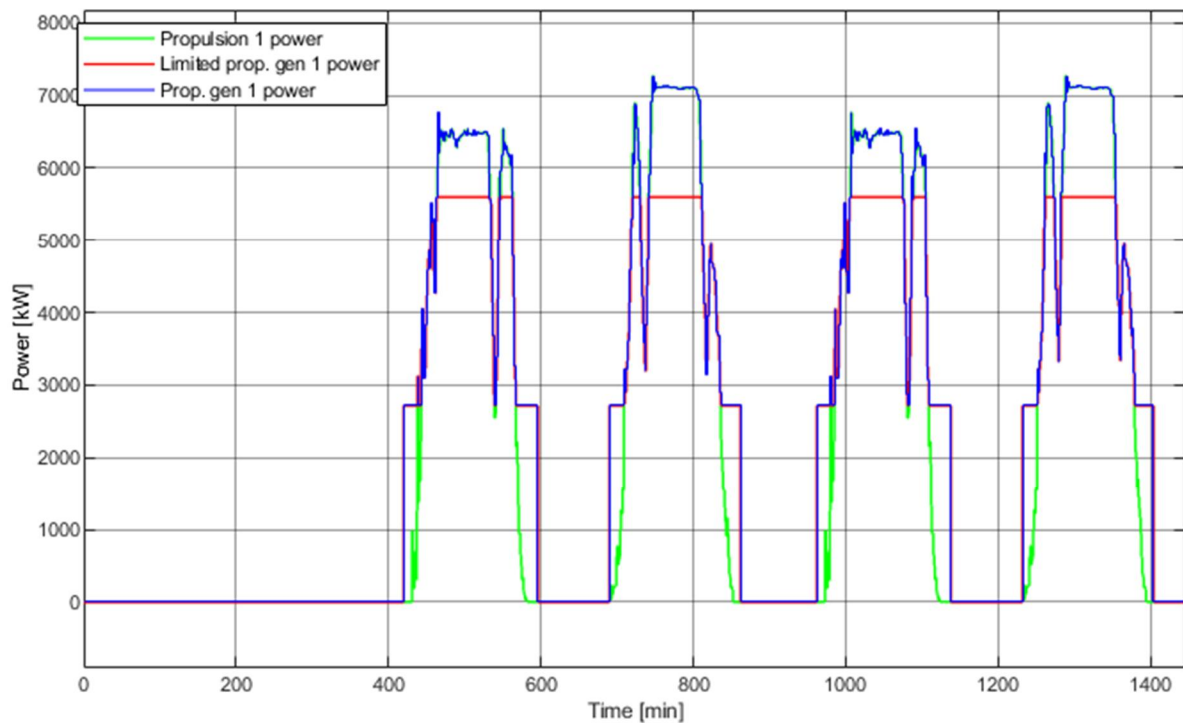


Figure 28. Propulsion generator 1 generated power, limited generated power and propeller 1 electrical load

With two propulsion generators running the 30 % loading generates approximately 5.5 MW peak power. The difference between propulsion power and propulsion generator loading is charged into the energy storage according to Figure 29.

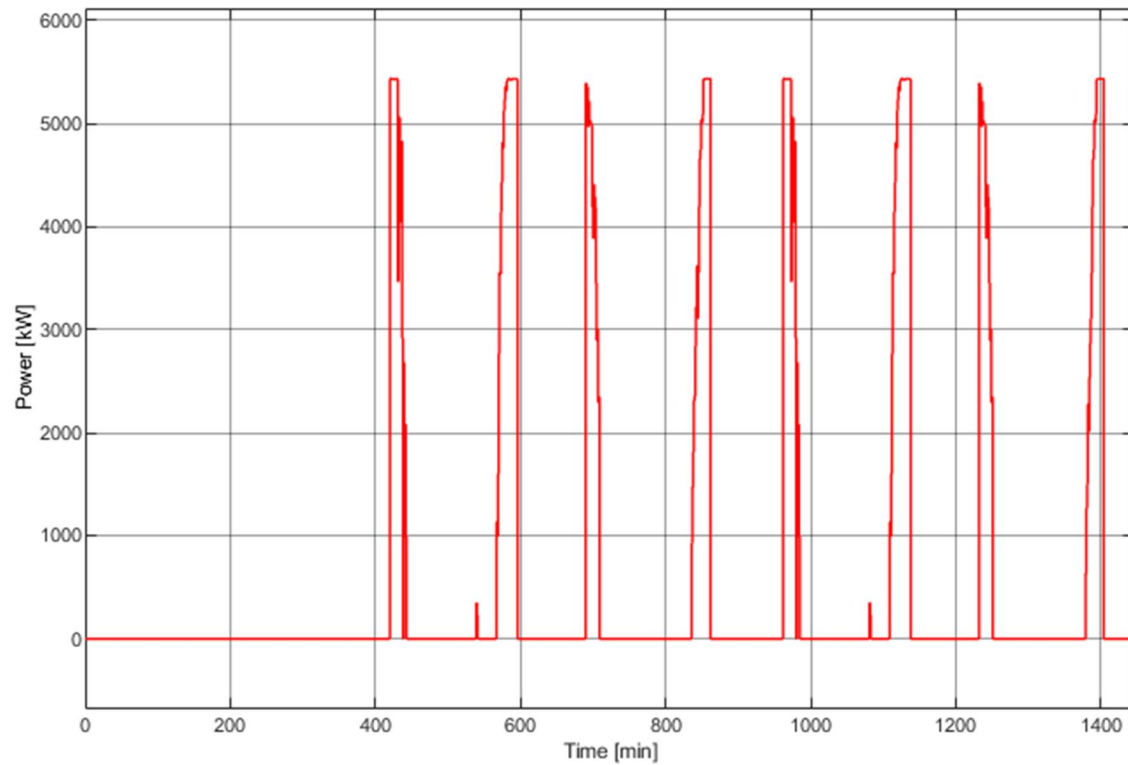


Figure 29. Charge cycle of the energy storage

The total energy of the charging cycles is approximately 14 MWh with peak power of 5.5 MW. The discharging power peaks shown in Figure 30 are not as high as the charging power peaks but the duration is longer.

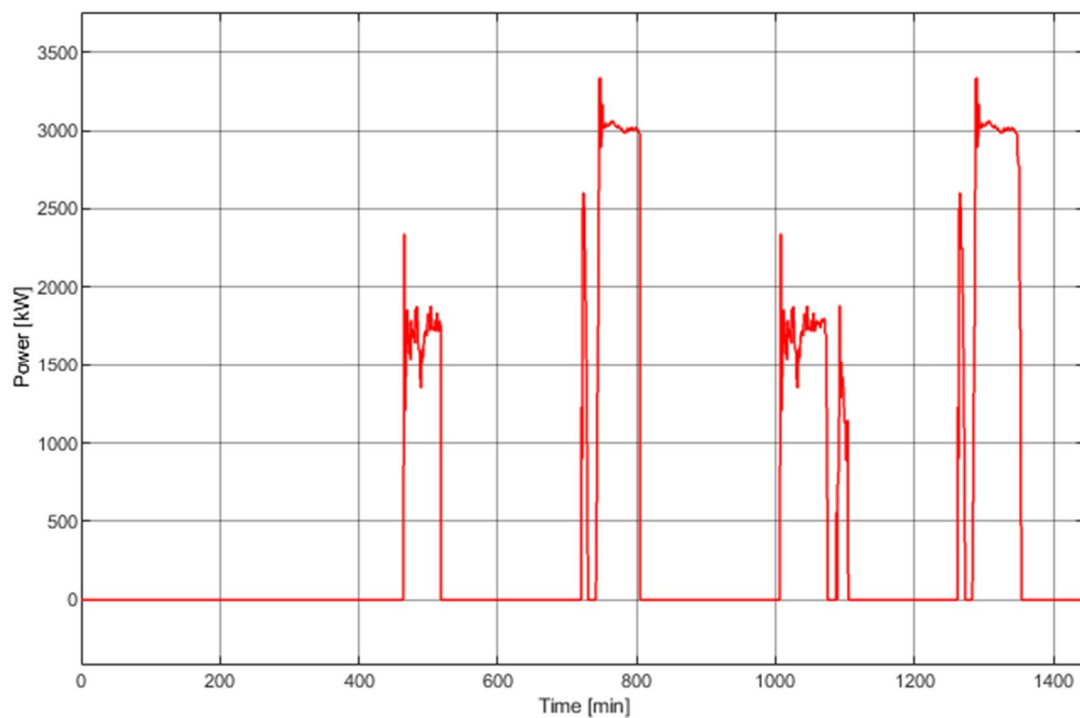


Figure 30. Discharge powers of energy storage

The discharging peaks are approximately 3.4 MW and the discharging energy is approximately 11.7 MWh. The capacity needed is around 5 MWh but to be able to operate in end of lifetime of the energy storage the capacity is needed to be 6 MWh. This also ensures that the charging peak powers are always under 1C which allows more battery technologies to be considered in operation. The C-rate can be calculated with equation

$$C = \frac{P}{E_{cap}} \quad (12)$$

where P is charge or discharge power and E_{cap} is total capacity of the energy storage (Miao, 2019). The simulation model is built according to Appendix 1. In the end of lifetime of the battery it is needed to ensure that the charging peaks are also under 1C to be able to operate batteries as planned. In the end of lifetime, the capacity is considered to be 80 % of the original which in this case means that the capacity of 6 MWh energy storage would be 4.8 MWh. The end of lifetime SOC behaviour with initial SOC of 50 % is shown in the Figure 31.

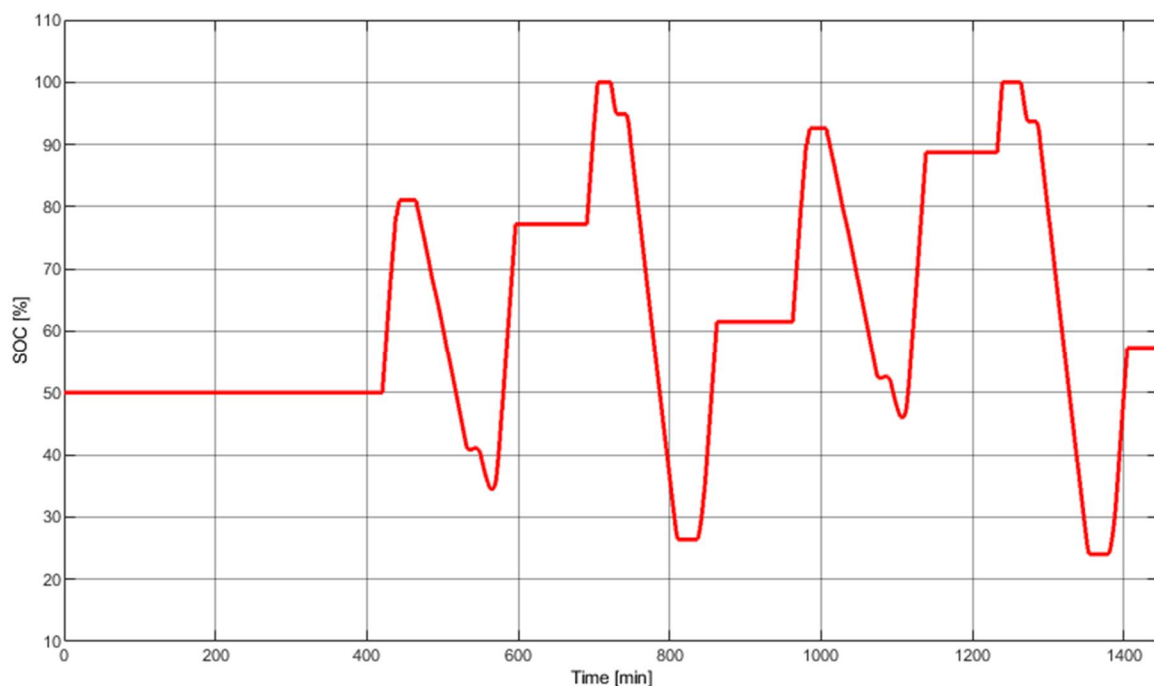


Figure 31. State of charge of 6 MWh battery in end of lifetime with 80 % capacity and 50 % initial charge

The 50 % initial charge is the best option since with these loading conditions all the charging and discharging possibilities are utilized. The 50 % charge should be target in the end of the day. When the initial charge is 100 % in Figure 32, not all the possible charging is utilized.

For example, the first peak in the first run of the day is not charged since the capacity is full already. This weakens the energy efficiency and has a slightly less fuel savings as calculated with 50 % initial charge since the excessive energy from the propulsion generators is not utilized.

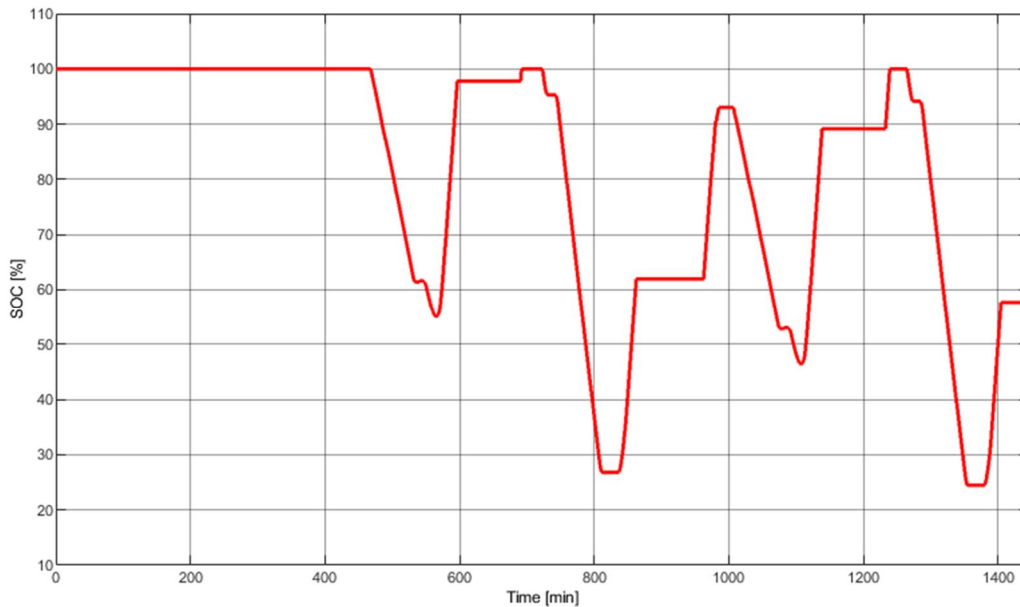


Figure 32. State of charge of 6 MWh battery in end of lifetime with 80 % capacity and 100 % initial charge

If the initial charge of the battery is 100 % the first charge beginning from 420 min and the peaks near 700 min and 1250 min are not utilized compared to Figure 31. Alternatively, if the initial SOC is at the safety limit of 20 % charge in Figure 33, not all the discharge opportunities are used.

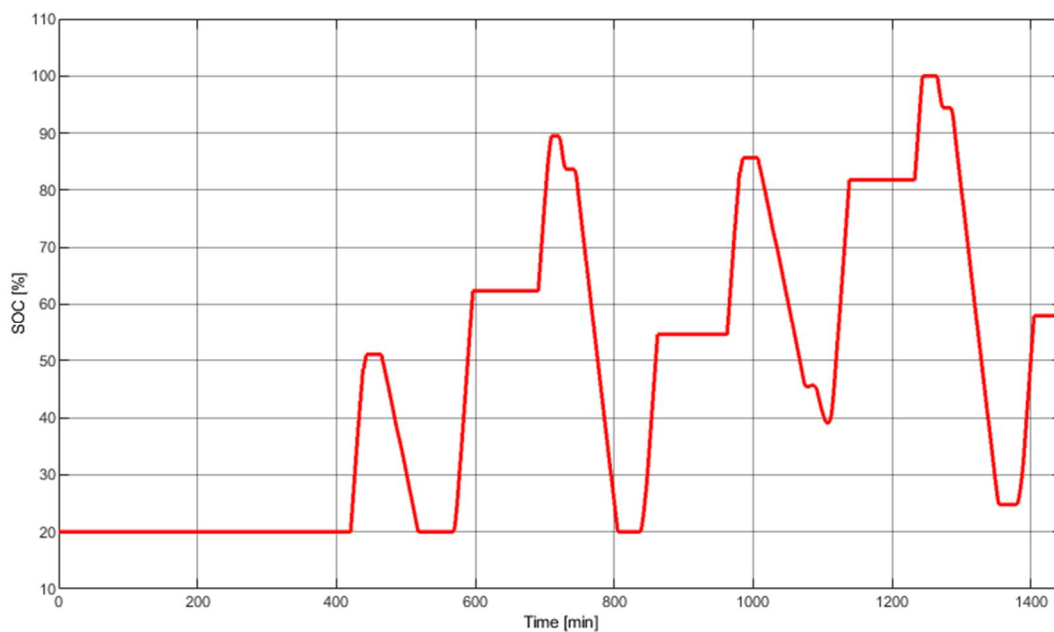


Figure 33. State of charge of 6 MWh battery in end of lifetime with 80 % capacity and 20 % initial charge

The energy storage energy waveform is the same as SOC waveform, but the scale is different as the 100% is 6 MWh and 20 % is 1.2 MWh in the beginning of lifetime. If the battery has been used down to 20 % state of charge in its last operation, all the charges are utilized but the SOC from 500 min onwards and from 800 onwards is dropped back to safety level of 20 % which leads to situation where the generator power is needed to rise in these occasions as we can see in the Figure 34.

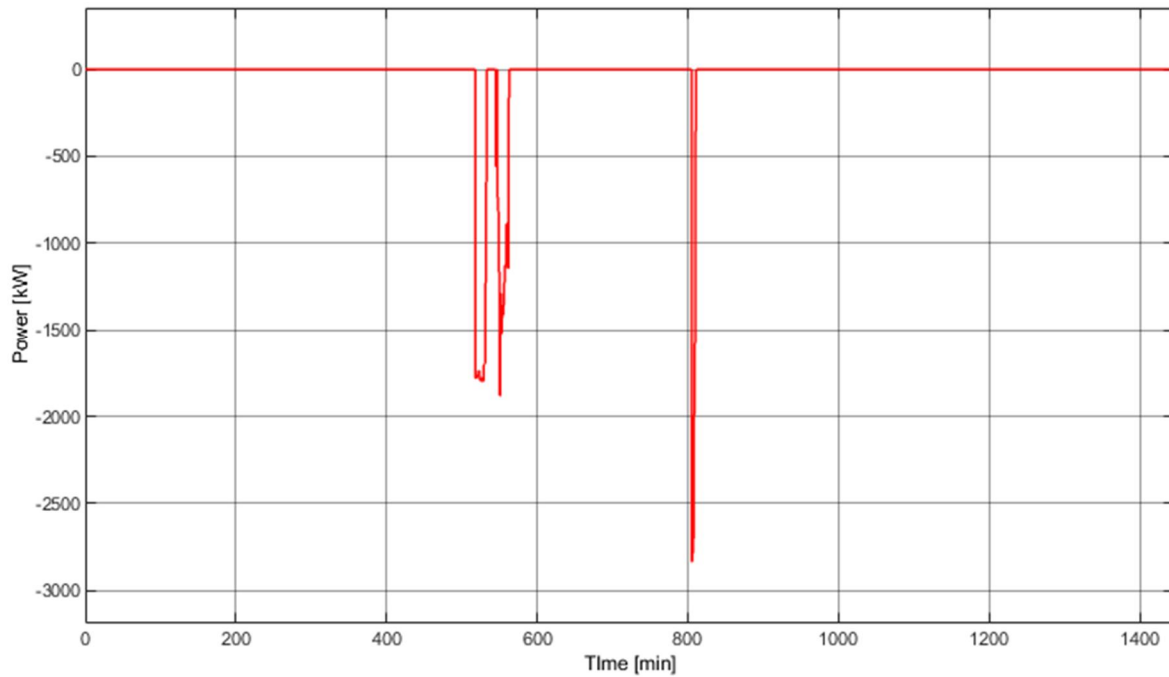


Figure 34. Deficit power caused by low battery charge

The total additional energy needed in the end of lifetime from the generators is 0.93 MWh if the initial SOC is 20 % compared to the initial SOC of 50 % where all the charge and discharge possibilities are utilized. With full capacity this energy would be 0.61 MWh. However, the operation conditions vary from day to day. Losses of operation is described in Figure 35.

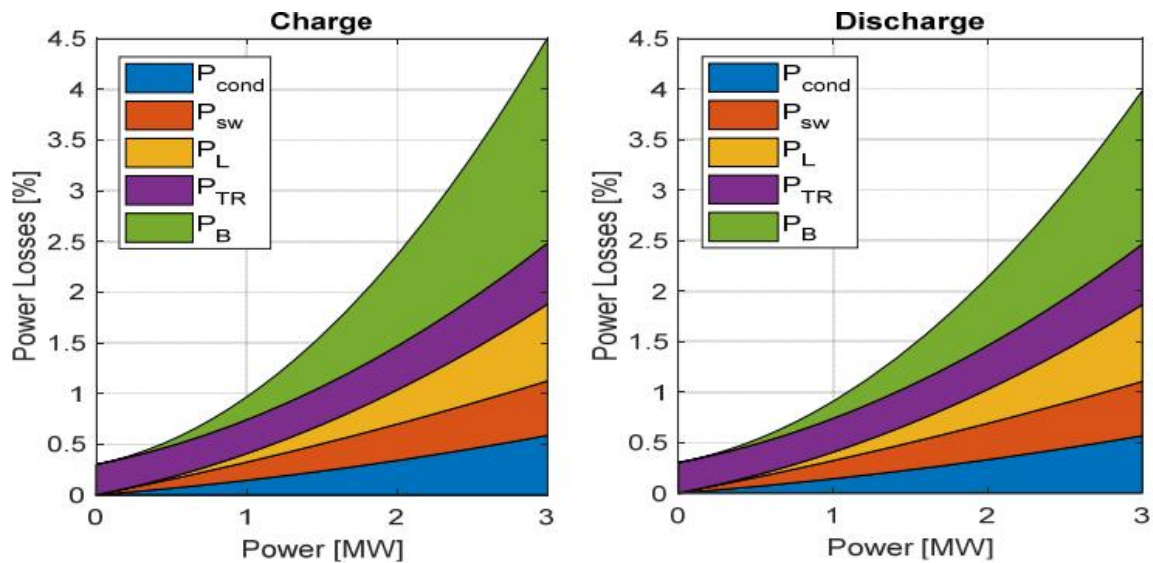


Figure 35. Losses from charging and discharging the energy storage, P_{cond} is conduction losses, P_{sw} is switching losses, P_L is filter induction losses, P_{TR} is transformer losses and P_B is battery array losses (Barrera-Cardenas, 2019)

To simplify the simulation model the power converter losses are neglected in this study since the efficiencies are high and the charged energy is in all cases over the discharge energies. For more detailed analysis with precise measurement data the losses are needed to take into account. The conditions in these calculations are considered to be average so in some days the benefit could be better than in some days.

5.3 Hotel load serving harbour operated energy storage

In this scenario the energy storage is used to replace one of the hotel loads serving generators and using the stored energy in harbour operation to avoid the pollutions near harbours for greener image. Propulsion generator energy production is identical to Figure 28, but the load is not limited in this scenario. In initial conditions the generator which is being replaced produces approximately 0.78 MWh of energy with power cycles of Figure 36.

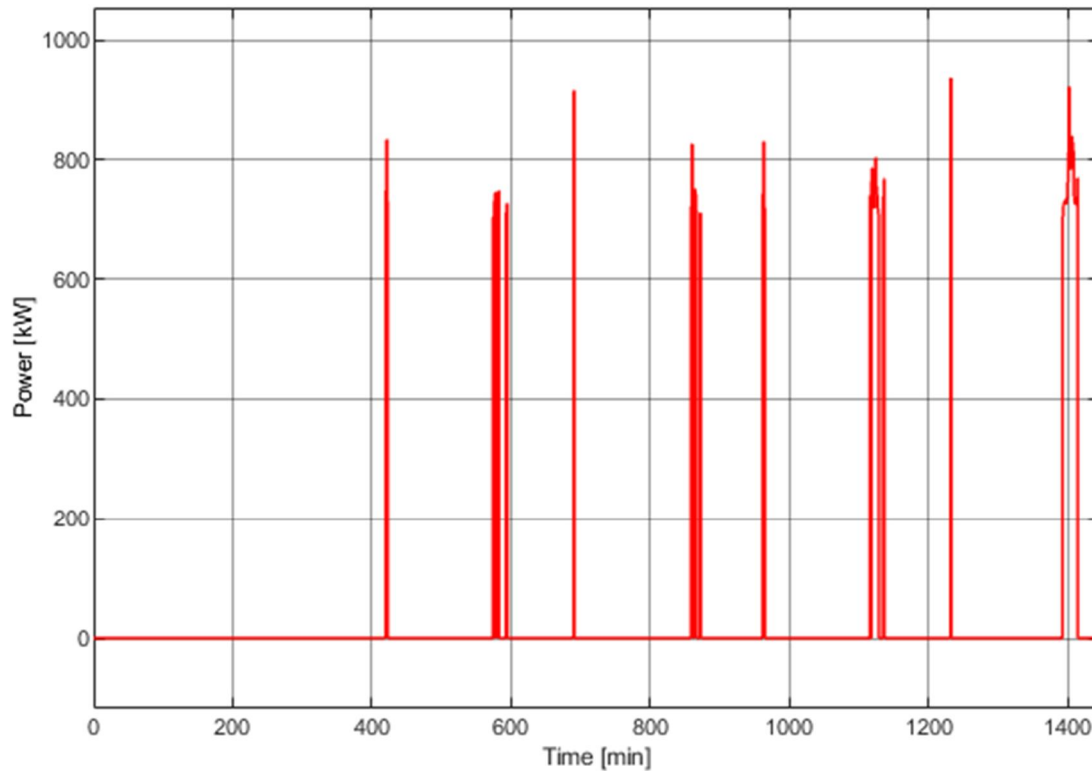


Figure 36. Hotel load generator 4 power production in initial conditions

Together with this replacement the energy storage is operated in harbour to supply hotel load so that the other hotel load generator can be shut down. However, the generator is not shut down for overnight since the energy storage would require a lot of energy to operate overnight. It is only used in daily operations during visits in harbour. The amount of energy needed from energy storage in this operation mode is 3.2 MWh when combined with the energy required caused by the replacement of generator 4. This is also the parameter for the energy storage capacity since there are the same amount of charging energy available, but the consumption need is not so high as in the propulsion load scenario. The total power output from the energy storage can be seen in Figure 37.

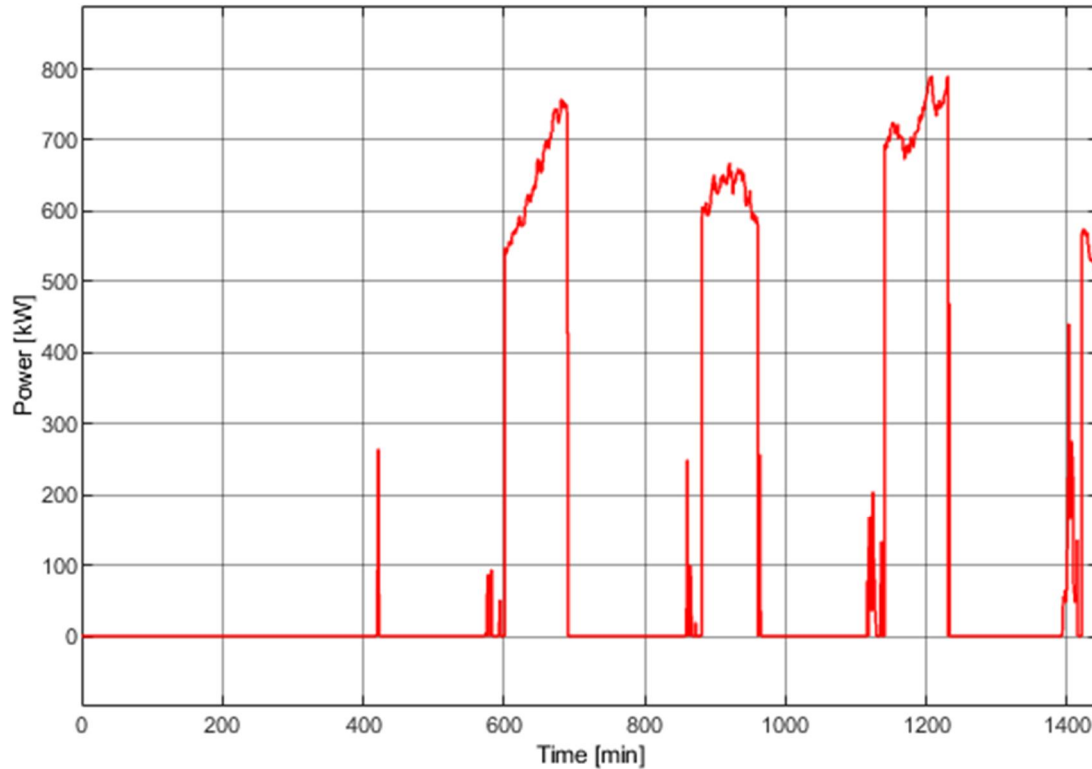


Figure 37. Energy storage power output in hotel load scenario

The maximum potential charged energy is approximately 13.9 MWh, but this would mean that the maximum charging power would be 5.5 MW as shown in Figure 29. That would mean that the energy storage battery cell technology would be needed to be designed so that the 5.5 MW charging can be utilized but when only under 0.8 MW discharge power is needed and only approximately 3.3 MWh energy needed from it, it is unnecessary to dimension the energy storage that large. Energy storage size is decided to be 2 MWh based on the simulation. It would be enough to charge with limited charging power of 1.1 MW which would equal in 3.5 MWh total energy and would exceed the required energy but with initial charge of 20 % in the beginning the cycle the required energy exceeds the available energy leading to SOC safety limit of 20 % charge (Figure 38).

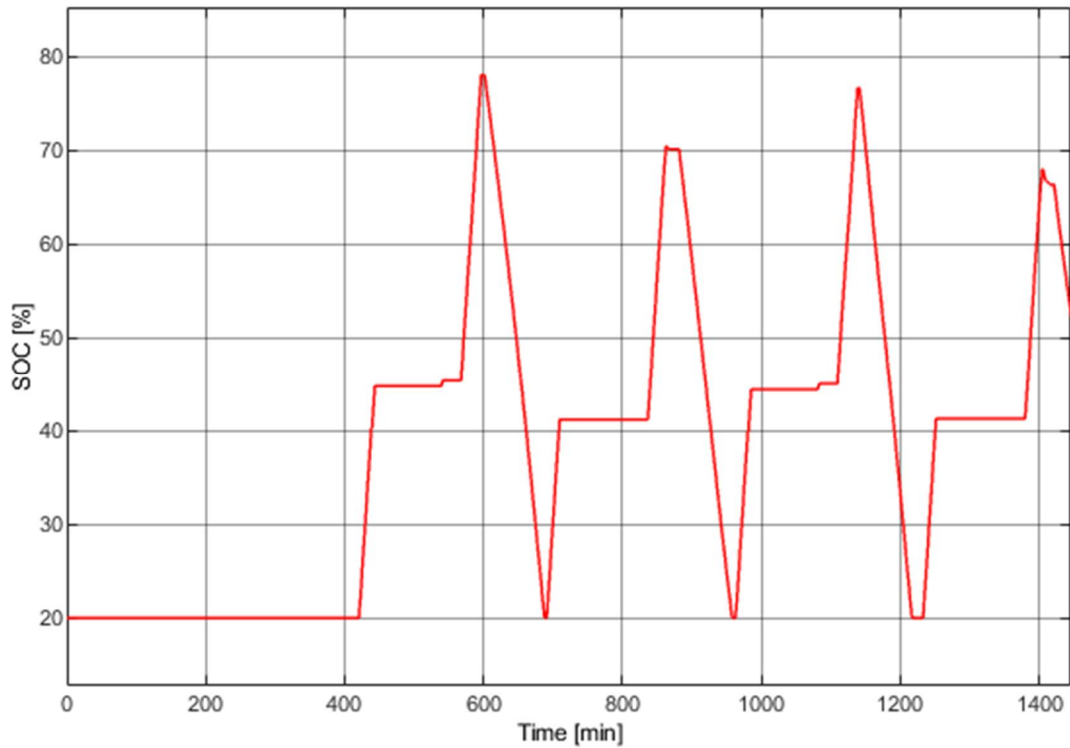


Figure 38. SOC with initial charge of 20 % in hotel load scenario

SOC drops to 20 % in under 700 min, 960 min and 1220 min. The power required during these times is shown in Figure 39.

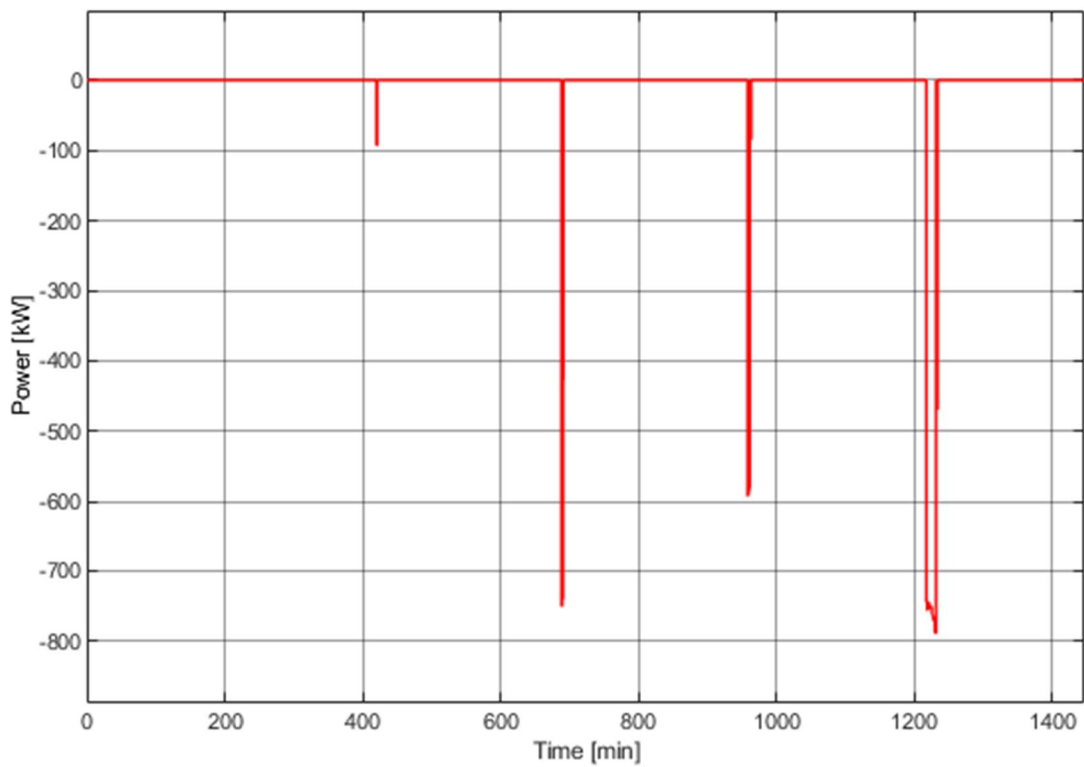


Figure 39. Deficit power caused by SOC drop to 20 % safety limit

The operated ship is in harbour during these power shortages. Compared to earlier scenario where the deficit power could be fixed with increasing generator supply, now the generators are not running so initial SOC of 20 % is not an option. However, if the controlling system requires the initial charge to be at least 50 % (Figure 40) when docking is predicted the operation with 1.1 MW charge could be worked out.

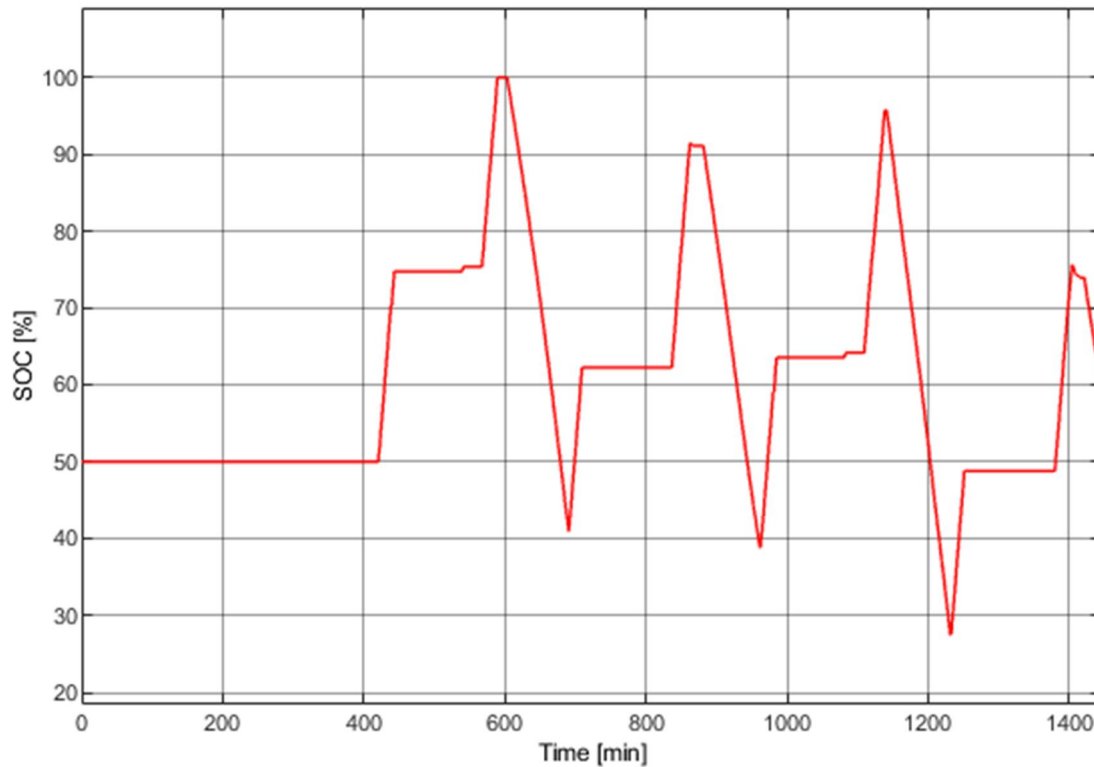


Figure 40. SOC with initial charge of 50 % in hotel load operation

The charging power can be also higher than 1.1 MW if required. However, the hotel load energy consumption in harbours should be easily predictable since the operating conditions have a very minimum effect on the energy consumption when docked.

5.4 Battery technology selections

The energy storages are dimensioned so that the operation is possible in 80 %. The capacity between 70 % to 80 % is considered to be end of lifetime in lithium-ion cells. Lithium-ion cells suffer from calendar aging which is considered to be at least 10 years in no load conditions and cyclic aging which depends on the cyclic usage of batteries. Equivalent full cycle (EFC) is the measurement of charge throughput which equals to two times of the capacity of a new battery. (Maheshwari, 2019)

All the necessary values from the simulation model are collected in Table 5.

Table 5. Energy storage charging and discharging operations

	Propulsion storage initial	Propulsion storage 80 % capacity	Hotel storage initial	Hotel storage 80 % capacity
Capacity [MWh]	6.0	4.8	2	1.6
Peak power, charge [MW]	5.5	4.8	1.1	1.1
Peak power, discharge [MW]	3.4	3.4	0.8	0.8
C-rate, charge	0.9	1	0.6	0.7
C-rate, discharge	0.6	0.7	0.4	0.5
Energy charged [MWh]	12.7	12.1	3.5	3.4
Energy discharged [MWh]	11.7	11.7	3.2	3.2
Available power [MW]	5.5			
Available energy [MWh]	14.0			
Daily equivalent full cycles	1.06		0.88	

In propulsion scenario the energy storage goes approximately 1.06 equivalent full cycles and in hotel load scenario 0.88 equivalent full cycles. The cyclic lifetime is estimated for everyday use with 365 days a year. While commercial energy storage manufacturers offer for example for NMC up to 15 000 cycles it is assumed that the cycling is done with very low loads and always on the most efficient operation point with change of SOC being very low. Those loading scenarios would not be possible in this study. Battery technologies are compared in Table 6.

Table 6. Comparison between battery technologies (Batteryuniversity, 2019 & Praeger, 2020)^(*)

Scenario		NCA	NMC	LFP	LTO
	EFC ^(*)	500	1000 - 2000	2000 - 4000	3000 - 7000
	Avg. Specific energy [Wh/kg] ^(*)	250	185	105	65
Propulsion 6 MWh	Cyclic lifetime [a]	1.3	2.6 - 5.2	5.2 - 10.4	7.8 - 18.1
	Mass [kg]	24 000	32 400	57 000	92 300
	Total cell price [M€]	1.74	2.10	2.94	5.04
Hotel load 2 MWh	Cyclic lifetime [a]	1.6	3.1 - 6.2	6.2 - 12.4	9.3 - 21.8
	Mass [kg]	8 000	10 800	19 000	30 800
	Total cell price [M€]	0.58	0.70	0.98	1.68

NCA has a very poor lifetime in both scenarios since it is lasting for only 1.6 years in daily use. It is the cheapest and lightest option but not very useful because of the poor cycle life. NMC battery pack is slightly heavier and expensive than NCA, but cyclic lifetime improves massively. In propulsion usage the 6 MWh battery pack lasts from 2.6 to 5.2 years and in hotel usage the 2 MWh pack lasts from 3.1 to 6.2 years. LFP has improved cyclic lifetime but is almost two times heavier than NMC. In 6 MWh pack the lifetime is expected to be from 5.2 years to 10.4 years and in 2 MWh pack from 6.2 years to 12.4 years. LFP is also more expensive than NMC or NCA. The best lifetime is in LTO battery pack which is expected to be from 7.8 to 18.1 years in 6 MWh pack and from 9.3 years to 21.8 years with 2 MWh pack. However, the calendar lifetime may limit the cyclic lifetime. LTO is also clearly the most expensive and heaviest option with almost three times mass compared to NMC and the price is also over to times compared to NMC.

The best options are NMC and LFP for the energy storage and it depends if the mass or cyclic lifetime advantages is preferred. The energy density will of course decrease when modules are made from cells and racks from modules. In marine use important factors are safety, price, lifetime, space requirement and weight. From these the NMC is cheaper and lighter but the LFP will last longer and is slightly safer choice. Both are considerable technologies for marine use and NMC is more common with higher production rate and availability in commercially ready racks. However, the share of NMC in battery chemistry market is predicted to decrease approximately from 60 % to 30 % in 2030 while the share of LFP grows from 10 % to over 30 % making it more attractive technology. (greentechmedia, 2020)

While LFP could be better option for the energy storage it is easier to find commercial NMC products for further inspection and that is why the NMC is selected for further inspection.

5.5 Space requirements for the energy storage

Energy storage space requirements is hard to estimate without ready commercial racks since multiple cells are placed in module and multiple modules to rack (Figure 41). The control electronics, safety gears and cooling reserves space and the volumetric energy density is decreased massively and gravimetric energy density significantly.

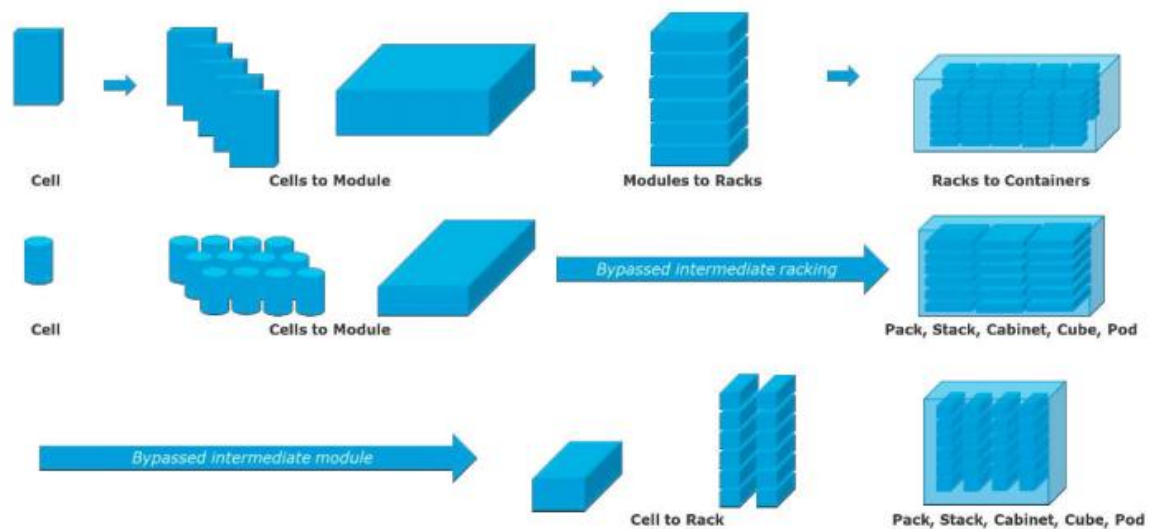


Figure 41. Battery cell transformation to energy storage (DNV GL, 2020)

For example, with NMC technology which cell chemistry is average of 185 Wh/kg the commercial solution has maximum gravimetric density of 110 Wh/kg. The volumetric density decrease is even larger because the racks need space between each other. Volumetric energy density is decreased from cell level of 325 Wh/L to 130 Wh/L which is 60 % decrease. (Corvus Energy, n.d.)

With module nominal capacity being 43 kWh and nominal voltage 76 V, the 1 kV voltage is reached with 14 modules in serial. This forms one string with capacity of 602 kWh and nominal voltage of 1075 V as announced in the technical details. Maximum voltage is 1142 V and minimum 1008 V, so the module voltage varies between 72 V and 82 V. Energy storage characteristics are shown in Table 7.

Table 7. Selected commercial energy storage characteristics (Corvus Energy, n.d.)^(*)

	Module ^(*)	Propulsion ESS	Hotel load ESS
Capacity [kWh]	43	6020	2408
Number of modules	1	140	56
Number of strings	-	10	4
Nominal voltage [V]	77	1075	1075
Max gravimetric density [Wh/kg]	110		
Max volumetric density [Wh/L]	130		
Mass [kg]	390	54600	21800
Floor area required [m ²]	-	25	10
Space required [m ³]	-	46	19

The system also requires inverters near the energy storage to convert the DC to AC. For the propulsion energy storage, the inverters are modular non-commercial bidirectional 1 MW inverters (Hercegfi, 2017) with AC and DC side protection and switchgears. After the DC is converted to AC it is necessary to rise the voltage up to the main bus voltage which in this case would be 6.6 kV. The size of inverter with switching gears and the size of transformers are estimated. Manufacturer claims that no service aisles are required but in this design there are 1000 mm service aisles. The energy storage, inverters and transformers can be located in various locations around the ship. One location could be near the main switchboards and main engines where the cabling distances are short, and the mass of the energy storage system would not unbalance the ship (Figure 42)

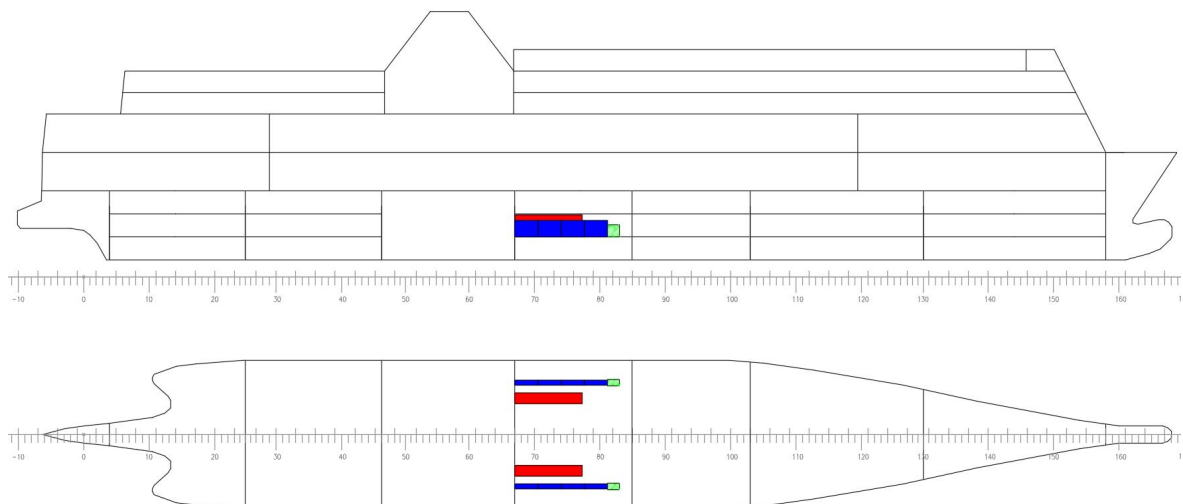


Figure 42. Propulsion energy storage of two 3 MWh placed in lower decks

The location however is in machinery spaces where usually the space reservations are crucial, and no extra space may be available at least in retrofits. In newbuild ships the arrangement of the machinery spaces in lower decks could be done the way that the energy storage has required space available. Fire safety and ventilation in this case is very important to build so that the system is safe to operate. However, the alternative solution could be to place the energy storage in the top decks outside where the system could be placed in containers if the IP-class is not high enough (Figure 43).

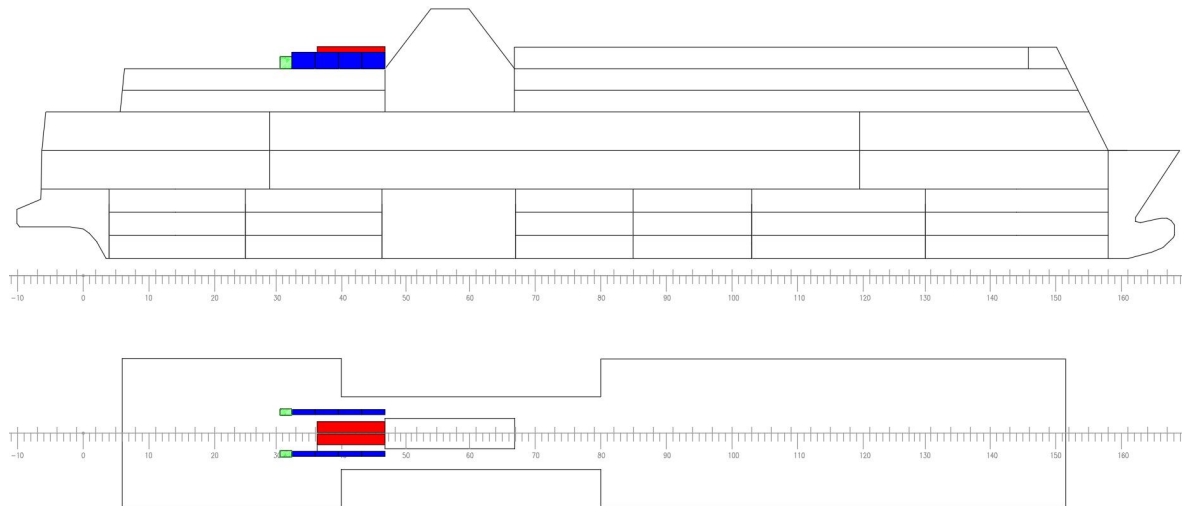


Figure 43. Propulsion energy storage of two 3 MWh placed in top decks

Cooling and ventilation are much cheaper to arrange, and the risk management is simplified. The downside of this arrangement is increased mass in the top decks causing raised center of mass and increased windage area. The hotel load energy storage could be placed in the same locations, but it would reserve less space. The problem in this solution is the large mass in the top of the ferry. This could make the operation unbalanced and before making this possible solution there should be mechanical calculations to ensure safe operation at sea. Also, the distance between the energy storage and main switchboard is longer in this placement causing more losses, voltage drop and higher cabling costs.

5.6 Fuel consumption

The energy storage operation allows lower operating hours for main engines which not only extends the lifetime of the engines but also has an effect in fuel consumption. The fuel consumption of Wärtsilä engines can be found in Wärtsilä engine configurator. The available values were for 100 %, 85 %, 75 % and 50 % loadings. Since there were only four measured points available from Wärtsilä engine configurator for used generators the 40 % generator

loading point specific fuel consumption is estimated value to get the third-degree interpolation line to fit the points. Since under 30 % loadings are not used the estimation is close enough for this purpose. Specific fuel consumptions for two different engine types and their fitted third-degree interpolation line is shown in Figure 44. (Wärtsilä, n.d. d)

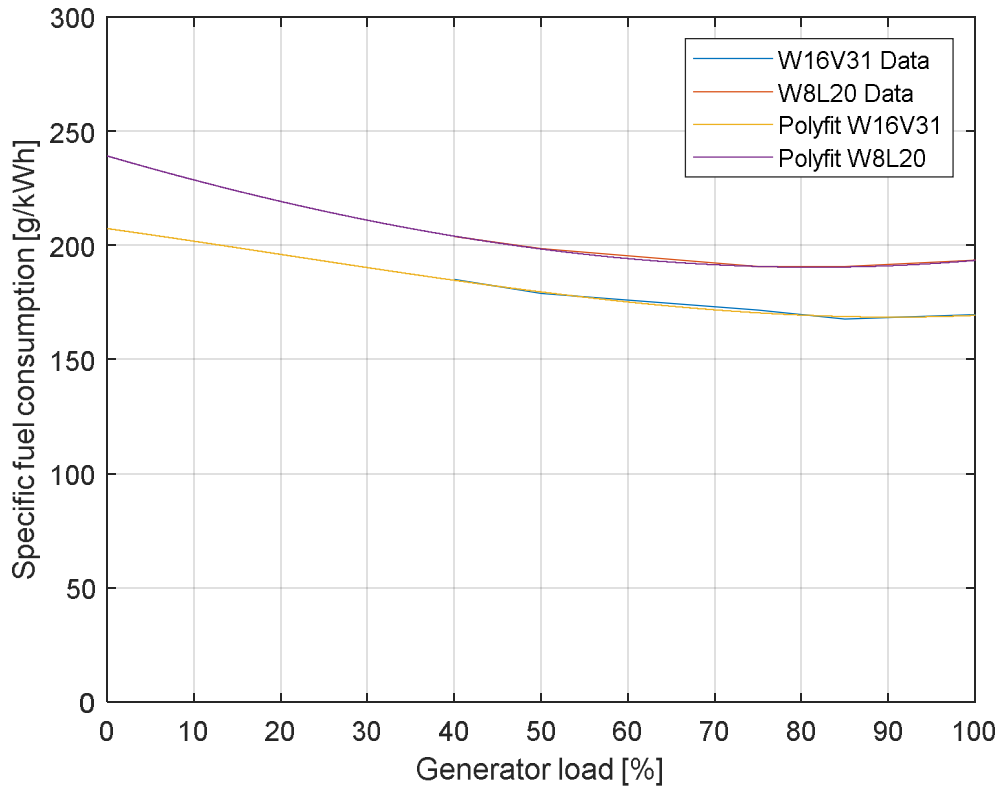


Figure 44. Estimated fuel consumption of the generator sets

The fuel consumption in tons can be evaluated with equation

$$FC = \sum \left(\frac{P \cdot SFC \cdot 1000 \text{ tons}}{60 \text{ min}} \right) \quad (13)$$

where P is power, SFC is specific fuel consumption, divider constant of 60 transforms the hours to minutes and 1000 kilograms to tons. When all the momentary fuel consumptions are added together the total fuel consumption for all the scenarios can be seen in Figure 45.

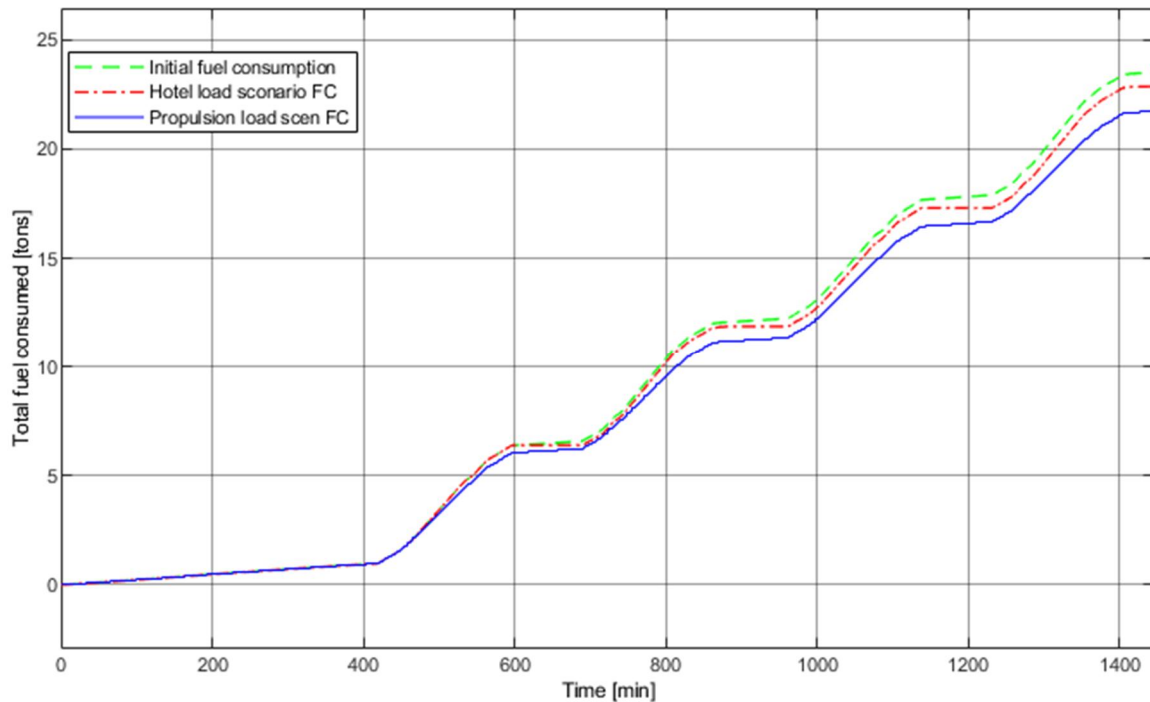


Figure 45. Total fuel consumption in initial conditions, hotel load scenario and propulsion load scenario

In initial conditions the daily fuel consumption were 23.52 tons. Using the energy storage in harbours for hotel load the fuel consumption dropped to 22.86 tons with saving being 0.66 tons and 2.8 % of the initial fuel consumption. In propulsion load scenario the fuel consumption dropped even more than in the hotel load scenario to 21.74 with savings of 1.78 tons and 7.6 % compared to initial consumption. Emissions are also reduced in proportion to fuel consumption. Of course, the weight is increased and the effect is slightly lower than calculated.

With very low sulphur fuel oil average price between 2019 and 2021 being 351 €/ton (Shipandbunker, n.d.) the fuel savings in hotel load scenario is approximately 230 €/day and 84 000 € yearly and in propulsion load scenario approximately 625 €/day and 228 000 € yearly.

5.7 Electrical distribution

In this project the radial power network is used since its more common and cheaper solution. The distribution network of the ferry is shown in Figure 46.

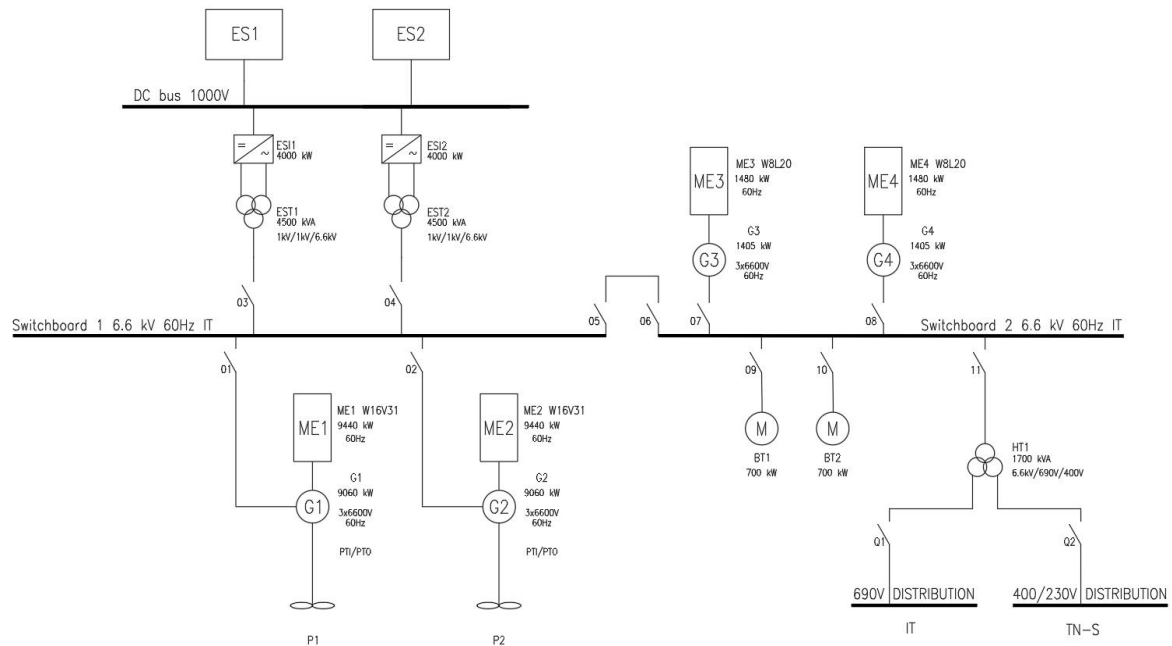


Figure 46. Electrical distribution single line diagram of the ferry

In the electrical distribution network, the main engines 1 and 2 are connected from shaft to power take out (PTO) / power take in (PTI) generator and straight to propellers. PTI/PTO generators are capable of feeding excessive energy to energy storages and vice versa taking energy from the energy storage to generator during lack of power.

In hotel load scenario the bus connectors between two switchboards are closed to be able to move power between them.

5.8 Cost estimation of the system

The cost of the system consists of many separate factors from which the main factors the energy storage itself, inverter, transformer, balance of plant, building- and commissioning costs. Balance of the plant includes all the auxiliary systems supporting the energy storage operation. For example, the ventilation, fire exhaustion and transformers belong to the balance of the plant. It also includes the cabling and connections at site. Cost estimation of the system is calculated in Table 8. (Mongird, 2019)

Table 8. Estimated cost of the system installed in the first time (Mongird, 2019)^(*)

	€/kW ^(*)	€/kWh ^(*)	6 MWh	2 MWh
Cost of energy		350	2.10	0.70
Power conversion system	200		1.20	0.40
Balance of plant	72		0.43	0.14
Construction and commissioning		80	0.48	0.16
Total cost [M€]			4.21	1.40

Assuming the battery packs are replaced every 5 years, inverters every 20 years, auxiliary systems every 40 years, commissioning costs being 50 000 € including maintenance and the cost of battery packs price being 20 % cheaper first two replacements the system would never pay itself back with only fuel savings as seen in Figure 47. The fuel price is estimated to grow 2 % annually until grown up to 40 % in 20 years. Only thing that could make the system profitable in some point is higher rise in the price of fuel or total replacement of one main engine where the main engine investment cost and operation and maintenance cost are saved.

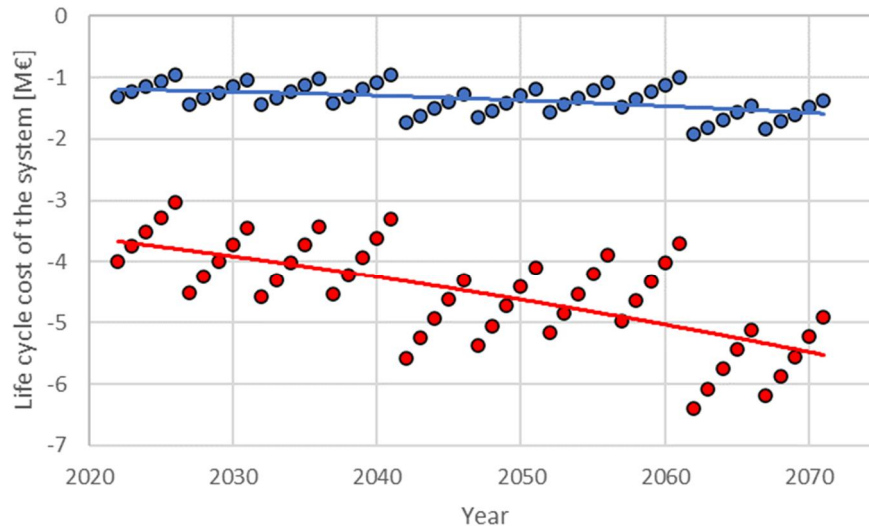


Figure 47. Life cycle cost analysis of the energy storage system

Operation of the system will cost money for the operator in this scenario. Therefore, with these parameters the whole system is not suitable for operation inspected in this study.

The zero-emission port mode can also be achieved with shore connection. This would be cheaper approach to operate in ports with no diesel engines running since the cost of the

connection would be only approximately 0.6 million euros for the ship and 1.2 million euros per terminal. The terminal build costs cannot be count for one ship only since at least in this route there are many operating ships, so the cost of terminal addition is divided. (Wbcsd, 2020)

6. CONCLUSIONS

The electrical energy consumption of the ferry consists mostly of propulsion load. Consumption is frequent with driving over 2 hours with almost full speed excluding the speed restriction zones and tight turns. Charging of the energy storage is mostly relatively short time peak powers with 5.5 MW power peaks lasting around ten minutes. This sets one dimensioning parameter for energy storage that it has to be able to withstand peak power at least 5.5 MW. Energy storage capacity was decided to be 6 MWh for propulsion usage and 2 MWh for hotel load usage based on the calculations where all charged energy is utilized.

The best battery technologies for the energy storage installed in ships are NMC and LFP based on the factors of cell price, gravimetric density, mass, cyclic lifetime and safety. LFP being even slightly better choice based on cyclic lifetime, but the lack of commercial solutions drives for choosing the NMC for more detailed analysis. LTO would have been cheaper in long run since it would not need to be replaced as often as NMC but LTO would have reserved much more space which would have been a problem. Even now with NMC technology the energy storage reserved a lot of space if located in lower decks taking space away from necessary systems related to ship operations. Moving it to top decks would unbalance the ferry so that there is a need for mechanical calculations before making it an option. The cost of NMC cells in 6 MWh energy storage is 2.1 M€ while the 2 MWh hotel load NMC cells cost only 0.7 M€.

The energy storage became unprofitable because of the long operation route and high power and the relative short life cycle. The saved fuel costs were not high enough to make the energy storage profitable. In harbour operation the shore connection would offer even more operation possibilities since the battery could be charged in ports also. The operation could then be in zero emission zones. The stored energy could be used while leaving the port and it would allow the ship to operate in low emission mode or emission free for a time being in sight of citizens. Shore connection was not part of this study but could be included in further simulations.

In energy storage capacity optimizing there are lots of parameters and there are also lots of parameters for the operation modes. In this study it has been decided to focus on propulsion usage to investigate the possibilities for hybrid propulsion and for hotel load use in harbours

with no shore connection to keep the emissions minimum near cities. The profitability could have been different with operation mode being dynamic positioning or thruster use. However, the initial data precision being one point per minute the estimation of this peak thruster loads and variable generator loading is hard.

Driver for the energy storage implementation could be either environmental or financial. While the system costs much compared to benefits the financial situation may change in the future if the fossil fuel price increase more than predicted in this study. Installation of the energy storage also lowers the operational and maintenance cost of the main engines which effect may be hard to estimate. Financially the energy storage presented in this study is not profitable and with presented parameters the system will never pay itself back. However, the cost of operation may not be barrier if the cost is not too high when other drivers are taken into account. The environmental driver could be greener image for the ship operator based on the fewer emissions and more sustainable operation. This can be caused also by socio-economic pressure toward shipowners. Technical drivers would also be part of financial ones since the main engine operation hours and maintenance costs are both technical and financial matters.

Energy storage brings most benefits out of it when it can either replace most of the main engines being either fully hybrid or hybrid propulsion ferry. In these cases, the savings from the main engine investments would cover at least part of the operation costs. The existing energy storages in ferries are placed in routes that are usually very short length and power much lower than in this study.

The result in this study shows that in general the large energy storages in medium distance travelling are hard to make profitable and even with different parameters and operation modes the payback time is probably so long that the whole investment is not financially wise to execute. For further analysis the shore connection possibility and different operation modes and operation distances could be investigated. However, the basic principle of the dimensioning remains the same but the parameters are the variables.

REFERENCES

- (ABB, 2004) ABB. 2004. *Akashia & Hamanasu - CRP Azipod propulsion*. [WWW]. [Accessed 06.04.2021]. Available online: <https://new.abb.com/marine/marine-references/shin-nikonhai-ferry-co>
- (ABB, n.d.) ABB. n.d. *Energy storage systems*. [WWW]. [Accessed 06.07.2021]. Available online: <https://new.abb.com/marine/systems-and-solutions/electric-solutions/energy-storage>
- (Ali, 2021) Ali, H., Jamil, F. & Babar, H. *Thermal Energy Storage – Storage Techniques, Advanced Materials, Thermophysical Properties and Applications*. ISBN 978-981-16-1130-8. Springer Nature, Singapore.
- (Andrea, 2010) Andrea, D. *Battery Management Systems for Large Lithium-Ion Battery Packs*. ISBN 978-1-60807-104-3. Artech house, Norwood, MA.
- (Barrera-Cardenas, 2019) Barrera-Cardenas, R., Mo, O. & Guidi, G. 2019. *Optimal Sizing of Battery Energy Storage Systems for Hybrid Marine Power Systems*. ISBN 978-1-5386-7561-8. IEEE Electric Ship Technologies Symposium (ESTS). Washington, DC, USA
- (Batteryuniversity, 2019) Batteryuniversity. *BU-205: Types of Lithium-ion*. [WWW]. [Last updated 10.07.2019] [Accessed 22.05.2021]. Available online: <https://batteryuniversity.com/article/bu-205-types-of-lithium-ion>
- (Berg, 2015) Berg, H. 2015. *Batteries for Electric Vehicles – Materials and Electrochemistry*. ISBN 978-1-107-08593-0. Cambridge university press, Cambridge.
- (Bureau Veritas, 2021) Bureau Veritas. 2021. *Rules for the Classification of Steel Ships - PART F – Additional Class Notations*. July 2021. Available online: https://erules.veristar.com/dy/data/bv/pdf/467-NR_PartF_2021-07.pdf
- (Bureau Veritas, 2018) Bureau Veritas. 2018. *Rules & Guidance notes - Power Generation Units. NR 656 DT R00*. Available online: https://erules.veristar.com/dy/data/bv/pdf/656-NR_2018-11.pdf
- (Camilo, 2006) Camilo, F. & Torresi, R. 2006. *Cathodes for Lithium Ion Batteries: The Benefits of Using Nanostructured Materials*. Available online:

- https://www.researchgate.net/publication/235587920_Cathodes_for_Lithium_Ion_Batteries_The_Benefits_of_Using_Nanostructured_Materials
- (Carlton, 2012) Carlton, J. S. 2012. *Marine Propellers and Propulsion*. 3rd edition. ISBN: 978-0-08-097123-0. Elsevier Ltd.
- (CAT, 2013) CAT. 2013. *The Impact of Generator Set Underloading*. [WWW] [Accessed 28.06.2021]. Available online: https://www.cat.com/en_US/by-industry/electric-power/Articles/White-papers/the-impact-of-generator-set-underloading.html
- (Corvus Energy, 2017) Corvus Energy. 2017. *Energy or Power – Corvus Energy Orca™ ESS Product Line Meets Both Differing Demands*. [WWW]. [Accessed 06.07.2021]. Available online: <https://corvusenergy.com/energy-or-power-corvus-energy-orca-ess-product-line-meets-both-differing-demands/>
- (Corvus Energy, n.d.) Corvus Energy. n.d. *Corvus Blue Whale*. [WWW]. [Accessed 03.08.2021]. Available online: <https://corvusenergy.com/products/corvus-blue-whale/>
- (DNV GL, 2020) DNV GL. 2020. *Energy - 2020 Battery performance scorecard*. Available online: <https://www.dnv.com/Publications/2020-battery-performance-scorecard-192180>
- (DNV GL, 2019a) DNV GL. 2019. *Rules for classification – Ships – Part 4 Systems and components – Chapter 8 Electrical installations*. Available online: <https://rules.dnv.com/docs/pdf/DNV/RU-SHIP/2019-10/DNVGL-RU-SHIP-Pt4Ch8.pdf>
- (DNV GL, 2019b) DNV GL. 2019. *Rules for classification – Ships – Part 6 Additional class notations - Chapter 2 Propulsion, power generation and auxiliary systems*. Edition July 2019. Available online: <https://rules.dnv.com/docs/pdf/DNV/RU-SHIP/2019-10/DNVGL-RU-SHIP-Pt6Ch2.pdf>
- (Espen, 2012) Espen, Ø. 2012. *Speed and powering prediction for ships based on model testing*. Master thesis in marine technology. Available online: <https://core.ac.uk/download/pdf/52099734.pdf>

- (European Commission, 2019) European Commission, 2019. *Reducing emissions from the shipping sector* [WWW]. [Accessed 12.02.2021]. Available online: https://ec.europa.eu/clima/policies/transport/shipping_en
- (ForSea, 2021) ForSea. 2021. *ForSea to upgrade Tycho Brahe with the world's largest battery pack, extending the vessel lifetime and cutting emissions.* [WWW]. [Accessed 05.08.2021]. Available online: <https://www.mynewsdesk.com/forsea/pressreleases/forsea-to-upgrade-tycho-brahe-with-the-worlds-largest-battery-pack-extending-the-vessel-lifetime-and-cutting-emissions-3112242>
- (Helsinki, 2018) Helsinki. 2018. *Kaupunkiympäristön julkaisuja 2018:25: Meriveden lämpötila Helsingin edustalla - Meriveden tyypillinen lämpötila pinta- ja pohjaläheisessä vedessä Helsingin edustan merialueella.* Available online: <https://www.hel.fi/static/liitteet/kaupunkiymparisto/julkaisut/julkaisut/julkaisu-25-18.pdf>
- (Hercegfi, 2017) Hercegfi, P. & Schönberger, S. 2017. *Modular and Compact IMW Inverter in one 19 " Rack for Storage and PV.* ISBN 978-3-8007-4424-4. PCIM Europe 2017, 16 – 18 May 2017, Nuremberg, Germany.
- (IEEE Spectrum, 2021) IEEE Spectrum. 2021. *The First Battery-Powered Tanker is Coming to Tokyo The "e5" vessel will use only lithium-ion batteries to ply Japan's coastline.* [WWW]. [Accessed 05.08.2021]. Available online: <https://spectrum.ieee.org/first-battery-powered-tanker-coming-to-tokyo>
- (Ilmatieteenlaitos, 2020) Ilmatieteenlaitos. Vuositilastot. [WWW]. [Accessed 25.04.2021]. Available online: <https://www.ilmatieteenlaitos.fi/vuositilastot>
- (Imarest, 2018) Imarest, institute of marine engineering, science & technology. 2018. *Norway creates world's first maritime zero emissions zone.* [WWW]. [Accessed 18.08.2021]. Available online: <https://www.imarest.org/themarineprofessional/item/4213-norway-creates-world-s-first-maritime-zero-emissions-zone>

- (IMO, n.d. a) IMO n.d. *Safety of ro-ro ferries*. [WWW]. [Accessed 05.08.2021]. Available online: <https://www.imo.org/es/OurWork/Safety/Paginas/RO-ROFerries.aspx>
- (IMO, n.d. b) IMO. n.d. *International Convention for the Safety of Life at Sea (SOLAS), 1974*. [WWW]. [Accessed 13.07.2021]. Available online: [https://www.imo.org/en/About/Conventions/Pages/International-Convention-for-the-Safety-of-Life-at-Sea-\(SOLAS\),-1974.aspx](https://www.imo.org/en/About/Conventions/Pages/International-Convention-for-the-Safety-of-Life-at-Sea-(SOLAS),-1974.aspx)
- (ITTC, 2008) ITTC. 2008. *ITTC – Recommended Procedures and Guidelines: Performance, Propulsion 1978 ITTC Performance Prediction Method. 7.5-02-03-01.4 - Revision 01*. Available online: <https://ittc.info/media/1593/75-02-03-014.pdf>
- (ITTC, 2011 a) ITTC. 2011. *ITTC – Recommended Procedures and Guidelines 7.5-02-02-01 - Revision 03*. Available online: <https://ittc.info/media/1217/75-02-02-01.pdf>
- (ITTC, 2011 b) ITTC. 2011. *ITTC – Recommended Procedures: Fresh Water and Seawater Properties. 7.5-02-01-03 - Revision 02*. Available online: <https://ittc.info/media/4048/75-02-01-03.pdf>
- (Jayasinghe, 2017) Jayasinghe, S., MEegahapola, L., Fernando, N., Jin, Z. & Guerro, J. 2017. *Review of Ship Microgrids: System Architectures, Storage Technologies and Power Quality Aspects*. MDPI Inventions (Basel), 2017-02-15, Vol.2 (1), p.4. Available online: <https://www.mdpi.com/2411-5134/2/1/4>
- (Komarnicki, 2017) Komarnicki, P., Lombardi, P. & Styczynski, Z. 2017. *Electric Energy Storage Systems – Flexibility Options for Smart Grids*. ISBN 978-3-662-53274-4. Springer-Verlag GmbH. Berlin, Germany.
- (Maheshwari, 2019) Maheshwari, A., Paterakis, N., Santarelli, M. & Gisbeascu, M. *Optimizing the operation of energy storage using a non-linear lithium-ion battery degradation model*. Elsevier Applied Energy Volume 261, 1 March 2020, 114360. Available online: <https://www.sciencedirect.com/science/article/pii/S0306261919320471>
- (Marineinsight, 2019) Marineinsight. 2019. *How The Power Requirement Of A Ship Is Estimated?*. [WWW]. [Accessed 08.05.2021]. Available online:

- <https://www.marineinsight.com/naval-architecture/power-requirement-ship-estimated/>
- (Marintek, 2004) Marintek. 2004. *Principal hull data – Hull model M2375J, Report 846001.20.01.*
- (Miao, 2019) Miao, Y., Hynan, P., Jouanne, A. & Yokochi, A. *Current Li-Ion Battery Technologies in Electric Vehicles and Opportunities for Advancements.* Available online: <https://www.mdpi.com/1996-1073/12/6/1074>
- (Molland, 2011) Molland, A. F., Turnock, S. R. & Hudson, D. A. 2011. *Ship Resistance and Propulsion – Practical Estimation of Ship Propulsion Power.* ISBN 978-0-521-76052-2. Cambridge University Press. New York.
- (Nitta, 2015) Nitta, N., Wu, F., Lee, J. & Yushin, G. *Li-ion battery materials: present and future.* Materialstoday Volume 18, Issue 5. Elsevier. Available online: <https://www.sciencedirect.com/science/article/pii/S1369702114004118>
- (Olabi, 2021) Olabi, A., Wilberforce, T., Abdelkareem, M. & Ramadan, M. *Critical Review of Flywheel Energy Storage System.* MDPI Energies 2021, 14(8), 2159.
- (Openseamap, 2021) Open sea maps. n.d. [WWW]. [Accessed 12.02.2021]. Available online: <https://map.openseamap.org/>
- (Oxford Institute, 2018) The Oxford Institute for Energy Studies. 2018. *Power-to-Gas: Linking Electricity and Gas in a Decarbonising World?* Oxford Energy Insight: 39. Available online: <https://www.oxfordenergy.org/wpcms/wp-content/uploads/2018/10/Power-to-Gas-Linking-Electricity-and-Gas-in-a-Decarbonising-World-Insight-39.pdf>
- (Papanikolaou, 2017) Papanikolaou, A., Skoupas, S., Zaraphonitis, G. & Boulougouris, E. 2017. *An integrated methodology for the design of RoRo passenger ships.* Available online: https://www.researchgate.net/publication/303298669_An_integrated_methodology_for_the_design_of_RoRo_passenger_ships
- (Preger, 2020) Preger, Y., Barkholtz, H., Fresquez, A., Campbell, D., Juba, B., Romàn-Kustas, J., Ferreira, S. & Chalamala, B. 2020. *Degradation of*

- Commercial Lithium-Ion Cells as a Function of Chemistry and Cycling Conditions*. Journal of The Electrochemical Society 167 120532. Available online: <https://iopscience.iop.org/article/10.1149/1945-7111/abae37>
- (Santhanagopalan, 2015) Santhanagopalan, S., Smith, K., Neubauer, J., Kim, G., Keyser, M. & Pesaran, A. 2015. *Design and analysis of large lithium-ion battery systems*. ISBN 978-1-60807-713-7. Artech house, Boston/London.
- (Scandlines, n.d.) Scandlines. n.d. *Our ferries and harbours*. [WWW]. [Accessed 12.02.2021]. Available online: <https://www.scandlines.com/about-us/our-ferries-and-harbours/>
- (Shagar, 2017) Shagar, V., Jayasinghe, S. G. & Enshaei, H., 2017. *Effect of Load Changes on Hybrid Shipboard Power Systems and Energy Storage as a Potential Solution: A Review*. ProQuest, Inventions, Vol. 2
- (Shipandbunker, n.d.) Shipandbunker. n.d. *Rotterdam bunker prices*. 11.07.2019-13.07-2021. [WWW]. [Accessed 14.07.2021]. Available online: <https://shipandbunker.com/prices/emea/nwe/nl-rtm-rotterdam>
- (Tallinna Sadam, 2020) Tallinna Sadam, 2020. *Port of Tallinn – Port Rules*. Available online: https://www.ts.ee/wp-content/uploads/2020/11/Sadama_eeskiri_2020_07_en.pdf
- (Väylävirasto, 2019) Väylävirasto, 2019. *Väyläkortti – Helsingin Länsisataman väylä*. Available online: <https://vayla.fi/palveluntuottajat/ammattimerenkulku/liikkuminen-vesivaylilla/vaylakortit>
- (Warner, 2015) Warner, J. 2015. *The Handbook of Lithium-Ion Battery Pack Design - Chemistry, Components, Types and Terminology*. XALT Energy, Midland, MI, USA. ISBN: 978-0-12-801456-1. Elsevier Inc.
- (Wbcsd, 2020) Wbcsd. 2020. *Shore-to-ship power*. Available online: https://wbcsd-publications.org/wp-content/uploads/2020/07/WBCSD_Business_Case_Shore_to_Ship.pdf
- (Weicker, 2014) Weicker, P. 2014. *A Systems Approach to Lithium-Ion Battery Management*. ISBN 978-1-60807-659-8. Artech house, Norwood, MA.

- (Wärtsilä, n.d. a) Wärtsilä, n.d. *Wärtsilä Built-UP Propellers*. [WWW]. [Accessed 12.04.2021]. Available online: <https://www.wartsila.com/marine/build/propulsors-and-gears/propellers/wartsila-built-up-propellers-bup>
- (Wärtsilä, n.d. b) Wärtsilä, n.d. *Encyclopedia of Marine Technology – Bow Thruster*. [WWW]. [Accessed 12.04.2021]. Available online: <https://www.wartsila.com/encyclopedia/term/bow-thruster>
- (Wärtsilä, n.d. c) Wärtsilä, n.d. *Encyclopedia of Marine Technology – Ship resistance*. [WWW]. [Accessed 12.04.2021]. Available online: <https://www.wartsila.com/encyclopedia/term/ship-resistance>
- (Wärtsilä, n.d. d) Wärtsilä, n.d. *Engine configurator*. [WWW]. [Accessed 14.07.2021]. Available online: <https://www.wartsila.com/marine/engine-configurator>
- (Wärtsilä, 2020) Wärtsilä, 2020. *Wärtsilä 31 Product guide*. Available online: <https://www.wartsila.com/marine/build/engines-and-generating-sets/diesel-engines/wartsila-31>

APPENDICES

Appendix 1. Simulation model

The simulation model is built so that the initial values of propulsion power, thruster power and hotel load is brought from external Excel-file from which the PMS receives the electrical loads. Propulsion generators 1 and 2 follow the propulsion load profile and while load being under 30% of the generation the exceeded power is charged to energy storage. Hotel load generators follow the load profile so that the generators 3 and 4 share the load when it exceeds the limit of one generator production. With low loads only one generator is running in hotel load and thruster side. Generators give feedback from power generation to PMS with output power and fuel consumption included. PMS gives output of total consumption, production and fuel consumption. The energy storage in this Figure 48 model feeds the propulsion load and in hotel load side the generator 4 is deleted and the PMS side control is changed so that the generator 3 is stopped in harbours and energy storage feeds the energy at the same time.

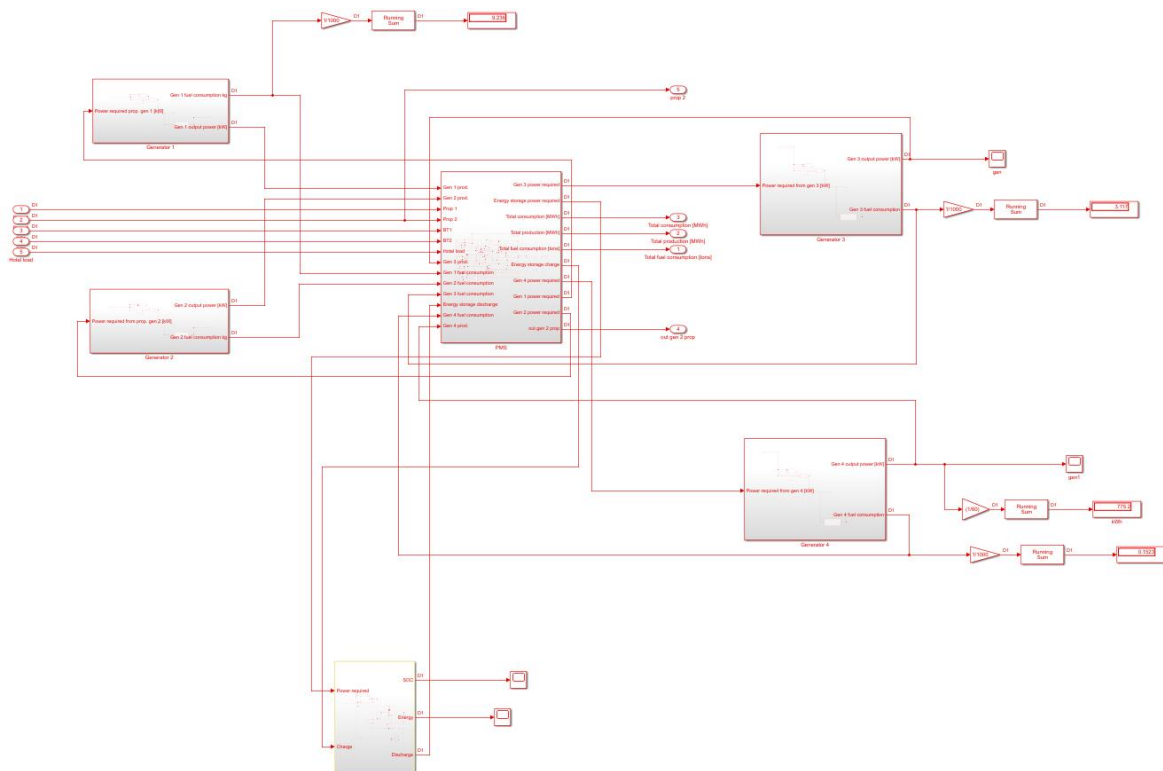


Figure 48. Simulation model of propulsion assistant energy storage

The energy storage is charged when generator 1 and 2 load is under 30 % of the produced energy and discharged when the limit of 5.6 MW is exceeded. The limit is set by daily and

can be adjusted during operation if something unpredicted occurs. In hotel load side the charging is done by same procedure, but the charging power is limited to 1.1 MW. This can also be adjusted but energy storage maximum charging rate must be taken into account. In the model the operation is predicted for the end of lifetime operation when 80 % of the capacity is available. In hotel load scenario the generators are shut down when docked and all the loads are fed from energy storage.